

## **FoP3B Part I Lecture 1: Free and nearly-free electron solids**

Electronic structure is fundamental to solid state physics. From the energies and distribution of electrons in solids it is possible to predict many physical properties, such as electrical, thermal conductivity, elastic stiffness, magnetism etc. Calculating the electronic structure for even a simple solid is however a formidable task, due to interactions between the many electrons and nuclei in the solid. It has taken well over a century for the theory to mature to the current state-of-the-art. A hierachal grouping of the different theories is given below. The first three theories are based on the *independent electron approximation*, where interactions between electrons in the solid are ignored (this can be partly justified using the Pauli Exclusion principle).

(i) Free electron theory: first proposed by Paul Drude in 1900 and based on the kinetic theory of gases. The electrons obey the classical Maxwell-Boltzmann distribution. Drude's theory successfully explained many experimental observations at the time, but there were also failures, notably the specific heat of electrons. In 1927 Arnold Sommerfeld used the newly developed quantum mechanics to replace the Maxwell-Boltzmann distribution with the Fermi-Dirac distribution, and obtained more accurate results. Apart from electron-electron interactions, the free electron theory also ignores interactions of the electrons with nuclei.

(ii) Nearly-free electron theory: here the electron-nuclear interaction is introduced using quantum mechanical perturbation techniques. Electron-nuclear interaction is crucial for explaining the electron behaviour close to the 'Brillouin zone boundaries'<sup>1</sup>. Because perturbation methods are used the theory is only valid for light atoms, where the electron-nuclear interaction is weak.

(iii) Bloch wave theory: developed by Felix Bloch this theory is valid for any electron-nuclear interaction regardless of its strength. The periodic property of crystals is exploited to analyse electronic structure.

(iv) Hartree Theory: developed by Douglas Hartree this theory was the first to include electron-electron interactions. It is the starting point for more advanced theories of electronic structure, such as density functional theory.

In this course we will only be covering the first three theories. Although not complete, it is still sufficiently advanced to enable a deep understanding of electrons in solids.

### ***Free Electron Theory***

It is important to first define what we mean by 'free electrons'. Figure 1a shows the structure of a free electron solid (e.g. a metal). The **ion cores** consist of positively charged nuclei and **bound electrons** that shield the positive charge from the rest of the solid. In between the ion cores are the **free electrons**, which are delocalised and can move throughout the solid. The material properties are largely governed by the free electrons and we therefore focus our attention on those electrons. For accurate results we need to treat the solid quantum mechanically and

---

<sup>1</sup> The Brillouin zone is at half the reciprocal vector spacing; the wavevectors within the Brillouin zone uniquely define the electron properties, such as energy.

therefore use the Fermi-Dirac distribution. Figure 1b shows that the Fermi-Dirac distribution is very different from the classical Maxwell-Boltzmann distribution. In particular, the electron energies are much higher in the former due the Pauli Exclusion principle, which only allows two electrons per electronic state.

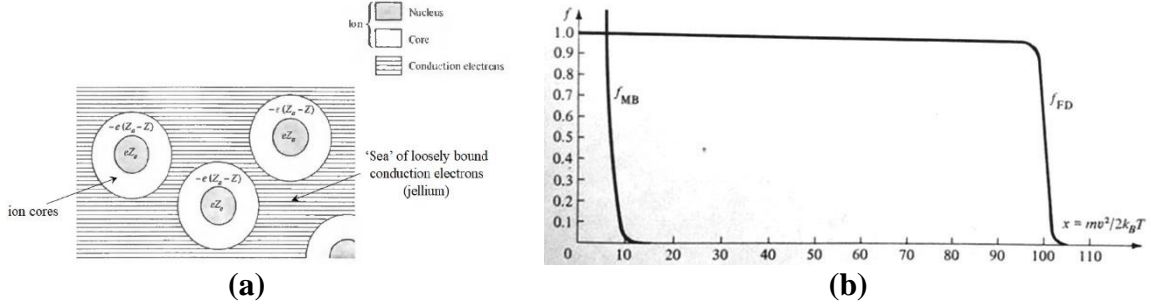


**Figure 1:** (a) structure of a free electron solid and (b) comparison of Maxwell-Boltzmann (MB) and Fermi-Dirac (FD) distributions.

The electrons must obey the Schrödinger equation  $\left(-\frac{\hbar^2}{2m}\nabla^2 + V\right)\psi = E\psi$ . For a free electron solid we assume that the potential energy  $V$  is constant and arbitrarily set it to zero (we are mainly interested in differences in energies, rather than absolute values). This can be justified by the fact that the bound electrons shield the nuclei and Coulomb interaction between the free electrons is minimised by the Pauli Exclusion principle. The electron wavefunction therefore takes the form of a plane wave  $\psi = \exp(i\mathbf{k} \cdot \mathbf{r})$  with energy  $E = \frac{(\hbar k)^2}{2m}$ .

The wavevector  $\mathbf{k}$  can only take discrete values due to the **boundary conditions**, which are defined for a travelling wave in the crystal (cf. standing wave solutions in the case of ‘particle in a box’ problem). Travelling waves are selected since we are interested in problems related to electrical, thermal conductivity etc where electrons travel over large distances. For a cube of length  $L$  the boundary conditions are  $\psi(x, y, z) = \psi(x + L, y + L, z + L)$ ; these are also known as *periodic boundary conditions*, since mathematically they are equivalent to a solid that is infinitely repeating. For a free electron wavefunction this results in  $\mathbf{k}$  vectors that are integer multiples of  $(2\pi/L)$  along any one of the  $x, y, z$ -directions. The volume of a  $\mathbf{k}$ -point in reciprocal space is therefore  $(2\pi/L)^3$  or  $(2\pi)^3$  per unit volume (i.e. cube of side length  $L=1$ ).

An important concept that will be useful later on is the **density of states**,  $g(E)dE$ , which is defined as the number of electronic levels between energies  $E$  and  $E+dE$  per unit volume of solid. For a free electron material  $E \propto k^2$  and therefore all states for a given energy will lie on a spherical surface in reciprocal space (see Figure 2). The density of states in reciprocal space  $g(k)dk$  is therefore equal to the volume of the thin shell (i.e.  $4\pi k^2 dk$ ) on the surface of the sphere divided by the volume of a single  $\mathbf{k}$ -point (i.e.  $(2\pi)^3$ ) with a factor of ‘2’ to take into account spin degeneracy (i.e. spin up and spin down electrons):

$$g(k)dk = 2 \frac{(4\pi k^2)dk}{(2\pi)^3}$$

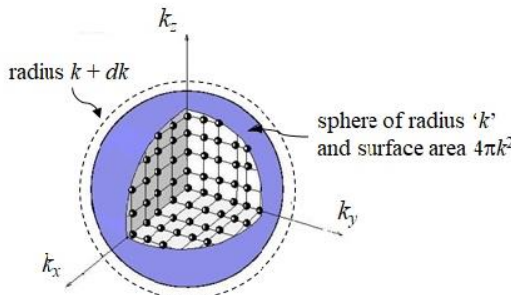


**Fig 2:** Fermi surface for an idealised free electron solid

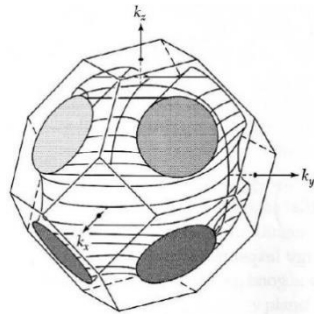


**Fig 3:** Fermi surface for copper

From  $E = \frac{(\hbar k)^2}{2m}$  we have  $\frac{dE}{dk} = \frac{\hbar^2 k}{m}$ , so that:

$$g(E) = \frac{1}{2\pi^2} \left( \frac{2m}{\hbar^2} \right)^{3/2} \sqrt{E}$$

Since energy must be minimised at absolute zero all electronic states within a sphere, also known as the **Fermi sphere**, will be fully occupied<sup>2</sup>. If  $k_F$  is the wavenumber of the Fermi surface (i.e. radius of the Fermi sphere in reciprocal space) it is easy to show that  $n = \frac{k_F^3}{3\pi^2}$ , where  $n$  is the electron density. Using copper as an example we can calculate  $n$  based on the valence of the atoms and lattice parameters of the unit cell. Hence  $k_F$ , and consequently energy of the electrons at the Fermi surface, can be determined. The Fermi energy in copper is  $\sim 7$  eV, equivalent to 81,290 K in temperature, with the electrons moving at  $\sim 1\%$  the speed of light! (cf. Fig 1b).

### Nearly-free electron model

Real materials do not always conform to the highly idealised free electron model. For example, the Fermi surface for copper is nearly spherical, but shows substantial deviations close to the Brillouin zone boundaries (Figure 3). Furthermore, the free electron model does not predict why some materials are electrical conductors and other insulators. To explain these phenomena, we need to take into account the electron-nuclear interactions, in what is called the *nearly-free electron theory*. Here we will only give a qualitative account, and reserve the quantitative description for the next lecture.

We can think of electron-nuclear interactions in terms of Bragg scattering of the electron plane waves from the crystal planes (Figure 4a). Constructive interference occurs when the path difference is equal to an integer number of wavelengths (i.e.  $n\lambda = 2ds\sin\theta$ ). This condition can also be expressed as  $(\mathbf{k}+\mathbf{G})^2 = k^2$ , where  $\mathbf{G}$  is a reciprocal vector. Here the Bragg diffracted beam has wavevector  $(\mathbf{k}+\mathbf{G})$  for incident wavevector  $\mathbf{k}$ . A potential solution is  $\mathbf{k} = -\mathbf{G}/2$ , so that the diffracted wavevector =  $+\mathbf{G}/2$ . There are now two plane waves in the crystal, an incident and Bragg diffracted wave, which can interfere with one another in one of two ways:

$$\begin{aligned}\psi(+)&= \exp(i\mathbf{G} \cdot \mathbf{r}/2) + \exp(-i\mathbf{G} \cdot \mathbf{r}/2) = 2\cos(\mathbf{G} \cdot \mathbf{r}/2) \\ \psi(-)&= \exp(i\mathbf{G} \cdot \mathbf{r}/2) - \exp(-i\mathbf{G} \cdot \mathbf{r}/2) = 2i\sin(\mathbf{G} \cdot \mathbf{r}/2)\end{aligned}$$

---

<sup>2</sup> At temperatures above 0 K some ‘smearing’ of the Fermi sphere takes place, due to the Fermi-Dirac distribution deviating from an ideal step function. However, the smearing is small, even at room temperature.

The first solution has maximum electron intensity  $|\psi(+)|^2$  at the positively charged nuclei which are potential wells. Therefore, the energy of  $\psi(+)$  is lowered. Conversely  $\psi(-)$  has maximum electron intensity between the nuclei and hence has higher energy (Figure 4b). Therefore, the electron energy becomes *non-degenerate* at the Brillouin zone boundary  $\mathbf{k} = \pm \mathbf{G}/2$ .

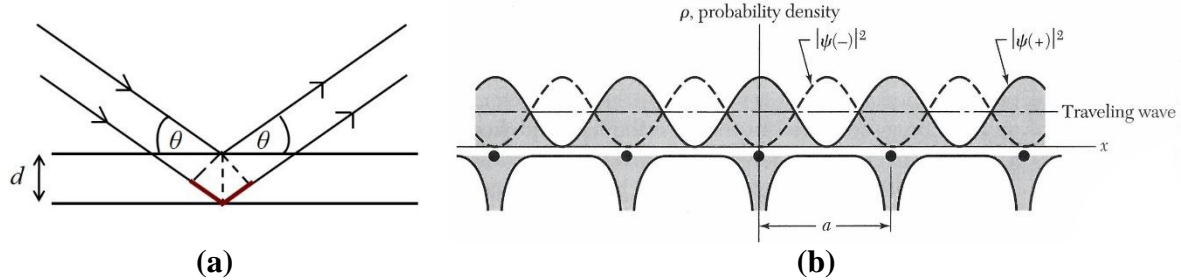


**Figure 4:** (a) Bragg diffraction from a crystal and (b) the two wave solutions at the Brillouin zone boundary

The **energy dispersion** (i.e.  $E$  vs  $k$ ) diagram for the free electron and nearly free electron models are shown in Figure 5. Note that the two curves are similar for small wavenumbers; it is only close to the Brillouin zone boundary, where the condition for Bragg diffraction is satisfied, that the two curves deviate from one another. In the nearly-free electron model there is a low and high energy band (i.e.  $\psi(+)/\psi(-)$ ) separated by a forbidden band or **band gap** which contains no electronic states. The electron group velocity  $v_g = \frac{d\omega}{dk} = \frac{1}{\hbar} \frac{dE}{dk}$  is also zero at the Brillouin zone boundary. This indicates that the electron forms stationary waves, as opposed to travelling planar waves, due to interference of the incident wave with its Bragg scattered wave.

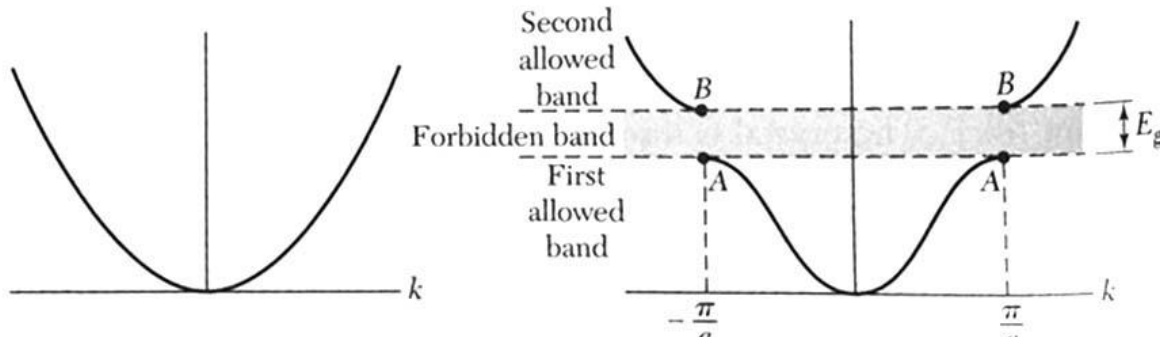


**Figure 5:** Energy dispersion curves for the free electron (left) and nearly-free electron models (right).

## FoP3B Part I Lecture 2: Energy band gaps

In this lecture we will develop the nearly-free electron model rigorously using quantum mechanical perturbation theory. Introducing the electron-nuclear potential energy ( $V_{\text{ion}}$ ) the Hamiltonian is modified to  $H = H_0 + V_{\text{ion}}$ , where  $H_0$  is the (free electron) unperturbed Hamiltonian, with plane wave solutions,  $\exp(i\mathbf{k}\cdot\mathbf{r})/L^{3/2}$ , for the electron eigenfunctions ( $L$  is the length of the solid cube and  $L^{3/2}$  is a normalisation constant). From *non-degenerate* perturbation theory the electron energy is:

$$E(\mathbf{k}) = E_0(\mathbf{k}) + \langle \mathbf{k} | V_{\text{ion}} | \mathbf{k} \rangle + \sum_{\mathbf{k}' \neq \mathbf{k}} \frac{|\langle \mathbf{k}' | V_{\text{ion}} | \mathbf{k} \rangle|^2}{E_0(\mathbf{k}) - E_0(\mathbf{k}')}$$
... (1)

Consider the numerator in the second order term.  $\langle \mathbf{k}' | V_{\text{ion}} | \mathbf{k} \rangle = \frac{1}{L^3} \int e^{i(\mathbf{k}-\mathbf{k}')\cdot\mathbf{r}} V_{\text{ion}}(\mathbf{r}) d\mathbf{r}$ , which is simply the Fourier transform of  $V_{\text{ion}}$  for reciprocal vector  $\mathbf{k}-\mathbf{k}'$ , i.e.  $V_{\mathbf{k}-\mathbf{k}'}$ . For crystals  $V_{\text{ion}}$  is periodic and therefore  $V_{\mathbf{k}-\mathbf{k}'}$  is only non-zero provided  $\mathbf{k}' = \mathbf{k} + \mathbf{G}$ , where  $\mathbf{G}$  is a reciprocal vector. Furthermore,  $\langle \mathbf{k} | V_{\text{ion}} | \mathbf{k} \rangle = V_0$ , which we can arbitrarily set to zero, as we did previously in the free electron theory. Therefore, the energy depends only on the second order term.

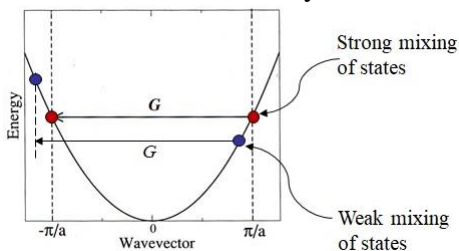


**Figure 1**

Figure 1 illustrates the mixing of two states with wavevectors separated by  $\mathbf{G}$ . For states away from the Brillouin zone boundary (e.g. the blue points), the energy difference is large, meaning that the second order correction is small (note that the energy difference appears in the denominator of the second order term). However, states close to the Brillouin zone boundary (red points) have similar energies and therefore show strong mixing.

States at the Brillouin zone boundary have identical energies, so that the second order correction diverges. *Degenerate* perturbation theory is therefore required for these states.

### Degenerate Perturbation Theory

Let two states  $|\mathbf{k}\rangle$  and  $|\mathbf{k}'\rangle$  be degenerate (i.e. have identical energy). The two states can interact to give a new state  $|\psi\rangle$  of energy  $E$ :  $|\psi\rangle = \alpha|\mathbf{k}\rangle + \beta|\mathbf{k}'\rangle$ . The linear coefficients  $\alpha, \beta$  and energy  $E$  are related by:

$$\begin{pmatrix} H_{11} & H_{12} \\ H_{21} & H_{22} \end{pmatrix} \begin{pmatrix} \alpha \\ \beta \end{pmatrix} = E \begin{pmatrix} \alpha \\ \beta \end{pmatrix}$$
... (2)

where the matrix element  $H_{ij} = \langle i | H | j \rangle$ , with  $|i\rangle, |j\rangle$  representing  $|\mathbf{k}\rangle$  and  $|\mathbf{k}'\rangle$  respectively. For the self-terms,  $H_{11} = \langle \mathbf{k} | H | \mathbf{k} \rangle = \langle \mathbf{k} | H_0 + V_{\text{ion}} | \mathbf{k} \rangle = \langle \mathbf{k} | H_0 | \mathbf{k} \rangle = E_0(\mathbf{k})$  and similarly  $H_{22} = \langle \mathbf{k}' | H | \mathbf{k}' \rangle = E_0(\mathbf{k}') = E_0(\mathbf{k})$ . The cross-term

$$H_{12} = \langle \mathbf{k} | H | \mathbf{k}' \rangle = \langle \mathbf{k} | H_0 + V_{\text{ion}} | \mathbf{k}' \rangle = \langle \mathbf{k} | V_{\text{ion}} | \mathbf{k}' \rangle = V_{\mathbf{k}'-\mathbf{k}}$$

(note that from  $H_0|\mathbf{k}'\rangle = E_0(\mathbf{k}')|\mathbf{k}'\rangle$ , it follows that  $\langle \mathbf{k}|H_0|\mathbf{k}'\rangle = E_0(\mathbf{k}')\langle \mathbf{k}|\mathbf{k}'\rangle = 0$ , due to orthonormality of  $|\mathbf{k}\rangle$  and  $|\mathbf{k}'\rangle$ ). Since  $\mathbf{k}' = \mathbf{k} + \mathbf{G}$ ,  $H_{12} = V_{\mathbf{k}' \cdot \mathbf{k}} = V_G$ . Similarly,  $H_{21} = \langle \mathbf{k}'|H|\mathbf{k}\rangle = V_{-\mathbf{G}} = V_G$  (since  $V_{\text{ion}}$  is real the Fourier coefficients must satisfy  $V_{-\mathbf{G}} = V_G$ ).

For non-zero values of  $\alpha, \beta$ :

$$\begin{vmatrix} H_{11} - E & H_{12} \\ H_{21} & H_{22} - E \end{vmatrix} = 0 \quad \dots (3)$$

which leads to two solutions for the energy given by  $E_{\pm} = E_0(\mathbf{k}) \pm |V_G|$ . Substituting in (2) results in  $\alpha = \pm\beta$ , so that the (normalised) wavefunction  $|\psi_{\pm}\rangle = \frac{1}{\sqrt{2}}(|\mathbf{k}\rangle \pm |\mathbf{k}'\rangle)$ . These results are identical to our qualitative description of the nearly-free electron theory in the previous lecture. In particular,  $|\psi_{\pm}\rangle$  has the same form as the wavefunctions constructed through interference of incident and Bragg diffracted waves at the Brillouin zone boundary. Furthermore,  $|\psi_{\pm}\rangle$  has different energies  $E_{\pm}$ , which are separated by a band gap of magnitude  $2|V_G|$  (see Figure 2).

Degenerate perturbation theory can also be extended to include  $|\mathbf{k}\rangle, |\mathbf{k}'\rangle$  states that are close to the Brillouin zone boundaries. Figure 2 depicts the situation for a 1D chain of atoms with periodic spacing  $a$  (the Brillouin zone boundary is therefore  $|\mathbf{G}/2| = \pm\pi/a$ ).

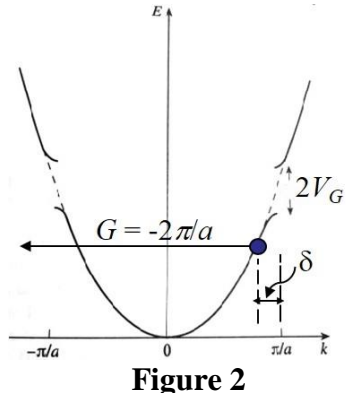


**Figure 2**

For  $k = (\pi/a) - \delta$  and  $k' = k + G = -\pi/a - \delta$ , it can be shown that for small  $\delta$ :

$$E_{\pm} = \frac{(\hbar\pi/a)^2}{2m} \pm |V_G| + \frac{(\hbar\delta)^2}{2m} \left[ 1 \pm \frac{(\hbar\pi/a)^2}{m|V_G|} \right]$$

Close to the Brillouin zone boundary the energy is a quadratic function of  $\delta$ , as plotted in Figure 2. Note that the gradient is zero at the Brillouin zone boundary, indicating the presence of standing waves with zero group velocity  $v_g = \frac{d\omega}{dk} = \frac{1}{\hbar} \frac{dE}{dk}$ .

### Band filling and Electrical conductivity

We will now examine the link between band filling and electrical conductivity. Consider again a 1D chain of  $N$  atoms with periodic spacing  $a$  (the length of the chain is therefore  $L = Na$ ). From the boundary conditions the spacing between  $\mathbf{k}$ -points is  $2\pi/L$ . The number of electronic states within the Brillouin zone of width  $(2\pi/a)$  is therefore  $2 \times (2\pi/a)/(2\pi/L)$ , where the factor of '2' is due to spin degeneracy. But  $2 \times (2\pi/a)/(2\pi/L) = 2L/a = 2N$ , i.e. there are twice as many electronic states within the Brillouin zone as there are atoms<sup>1</sup>. Therefore, for monovalent atoms the Brillouin zone is only half full, meaning that electrons can move under an electric field, since there are empty, higher energy states to which they can be easily promoted to. This explains why Group I metals, such as sodium and potassium, are good conductors. However, if the atoms are divalent the first Brillouin zone is completely full, and the unoccupied levels

<sup>1</sup> The result holds for 3D solids as well, except for 3D the number of electronic states is twice the number of primitive unit cells.

are separated by a band gap, i.e. there is an activation barrier. Therefore, Group II elements must be insulators, although this is inconsistent with the fact that metals such as calcium and magnesium are, in fact, good electrical conductors.

The reason for the discrepancy is because we have been considering 1D solids. Real materials are 3D, but we can resolve the discrepancy by analysing the simpler 2D case instead. Consider a 2D solid consisting of atoms periodically arranged in a square lattice. The reciprocal lattice points and first, second Brillouin zones are shown in Figure 3a, along with the Fermi surface as predicted by free electron theory (recall that since  $E \propto k^2$  for free electrons the Fermi surface is a circle). There are occupied energy levels within both the 1<sup>st</sup> and 2<sup>nd</sup> Brillouin zones. Now consider the energy gap at the first Brillouin zone boundary arising from nearly-free electron theory (Figure 3b). If the energy gap  $2V_G$  is large it is energetically unfavourable to have electrons in the 2<sup>nd</sup> Brillouin zone, so that these electrons must be transferred to the 1<sup>st</sup> Brillouin zone. After transfer the 1<sup>st</sup> Brillouin zone will be completely full, and since there is a large energy gap separating the occupied and unoccupied states, the material will be insulating. However, if  $V_G$  and the band gap is small, only *some* of the electrons in the 2<sup>nd</sup> Brillouin zone will be transferred to the 1<sup>st</sup> Brillouin zone (note the energy reduction due to electron transfer must be greater than the energy gain due to occupying states of larger wavenumber  $k$  within the 1<sup>st</sup> Brillouin zone). There are now occupied and unoccupied states within both 1<sup>st</sup> and 2<sup>nd</sup> Brillouin zones, meaning that electrical conduction can take place from electrons within both zones. This is consistent with electrical conductivity in divalent metals.

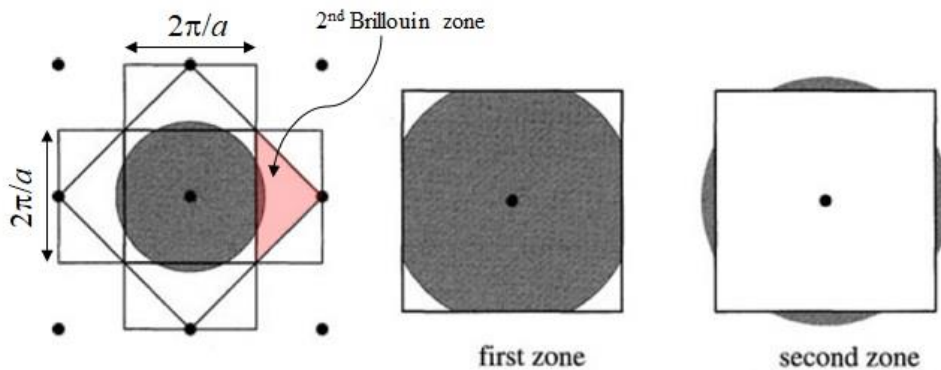


**Figure 3a:** reciprocal lattice and 1<sup>st</sup>, 2<sup>nd</sup> Brillouin zones for a divalent square lattice. The shaded circle represents occupied energy states, as predicted by free electron theory.

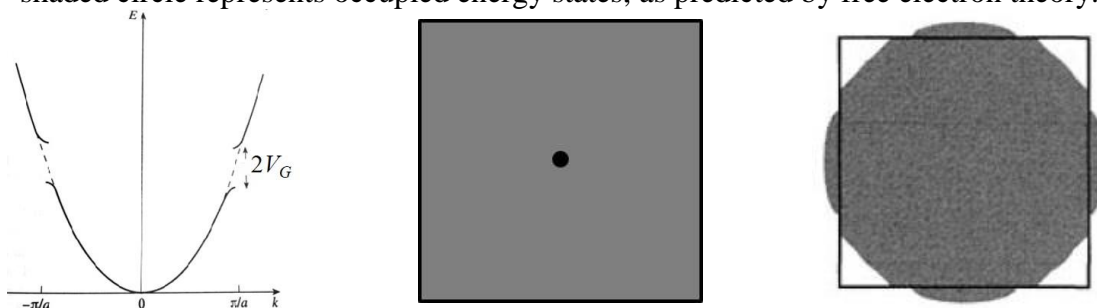


**Figure 3b:** (left) band gap at the Brillouin zone boundary. If the band gap is large it is energetically favourable for all electrons to occupy the 1<sup>st</sup> Brillouin zone causing it to be completely full (middle). For smaller band gaps only part of the electrons will be transferred from 2<sup>nd</sup> to 1<sup>st</sup> Brillouin zones (right; compare with Fig 3a).

## FoP3B Part I Lecture 3: Bloch waves

Consider the electron mean free path  $\lambda$  in a crystal, i.e. the average distance an electron travels before being scattered by an atomic nucleus.  $\lambda = v_F \tau$ , where  $v_F$  is the speed of Fermi surface electrons and  $\tau$  is the average collision time. From the first lecture  $v_F \sim 1\%$  speed of light and  $\tau$  for a metal such as copper is  $\sim 10^{-15}$ s. This gives  $\lambda \sim 10$  Å, which is several times larger than the average spacing between the atoms ( $\sim 1-2$  Å). How can this be? In this lecture we will develop **Bloch wave theory**, which explains the apparent anomaly. Unlike nearly-free electron theory, Bloch wave theory is valid for electron-nuclear interactions of any strength.

### **Bloch wave theory**

An electron in a solid must satisfy Schrödinger's Equation  $\left(-\frac{\hbar^2}{2m}\nabla^2 + V(\mathbf{r})\right)\psi(\mathbf{r}) = E\psi(\mathbf{r})$ .

Here  $V(\mathbf{r})$  is the total potential energy, i.e. it includes electron-electron and electron-nuclear interactions. For a crystal  $V(\mathbf{r})$  is periodic and can therefore be written as a Fourier series:

$$V(\mathbf{r}) = \sum_{\mathbf{G}} V_{\mathbf{G}} e^{i\mathbf{G}\cdot\mathbf{r}} \quad \dots (1)$$

Assume the wavefunction has the form ( $\mathbf{k}$  is the wavevector and  $C_{\mathbf{G}}$  are constants that are functions of  $\mathbf{k}$ ):

$$\psi_{\mathbf{k}}(\mathbf{r}) = \sum_{\mathbf{G}} C_{\mathbf{G}}(\mathbf{k}) e^{i(\mathbf{k}+\mathbf{G})\cdot\mathbf{r}} \quad \dots (2)$$

Substituting in the Schrödinger's Equation gives:

$$\sum_{\mathbf{G}} \left( \frac{\hbar^2}{2m} |\mathbf{k} + \mathbf{G}|^2 - E \right) C_{\mathbf{G}} e^{i(\mathbf{k}+\mathbf{G})\cdot\mathbf{r}} + \sum_{\mathbf{G}, \mathbf{G}'} C_{\mathbf{G}} V_{\mathbf{G}} e^{i(\mathbf{k}+\mathbf{G})\cdot\mathbf{r}} e^{i\mathbf{G}'\cdot\mathbf{r}} = 0 \quad \dots (3)$$

We can simplify the expression by making the substitution  $\mathbf{G} \rightarrow \mathbf{G} - \mathbf{G}'$  in the second summation:

$$\begin{aligned} & \sum_{\mathbf{G}} \left( \frac{\hbar^2}{2m} |\mathbf{k} + \mathbf{G}|^2 - E \right) C_{\mathbf{G}} e^{i(\mathbf{k}+\mathbf{G})\cdot\mathbf{r}} + \sum_{\mathbf{G}, \mathbf{G}'} C_{\mathbf{G}-\mathbf{G}'} V_{\mathbf{G}} e^{i(\mathbf{k}+\mathbf{G})\cdot\mathbf{r}} = 0 \\ & \text{or } \sum_{\mathbf{G}} \left\{ \left( \frac{\hbar^2}{2m} |\mathbf{k} + \mathbf{G}|^2 - E \right) C_{\mathbf{G}} + \sum_{\mathbf{G}'} C_{\mathbf{G}-\mathbf{G}'} V_{\mathbf{G}'} \right\} e^{i(\mathbf{k}+\mathbf{G})\cdot\mathbf{r}} = 0 \end{aligned} \quad \dots (4)$$

The above must be valid at all points  $\mathbf{r}$  in the crystal, so that the term within the curly brackets must be zero. This gives the so-called **characteristic equation** for Bloch waves:

$$\left( \frac{\hbar^2}{2m} |\mathbf{k} + \mathbf{G}|^2 - E \right) C_{\mathbf{G}} + \sum_{\mathbf{G}'} C_{\mathbf{G}-\mathbf{G}'} V_{\mathbf{G}'} = 0 \quad \dots (5)$$

We can write down a characteristic equation for each  $\mathbf{G}$ , so that Equation 5 represents a set of simultaneous linear equations linking the  $C_{\mathbf{G}}$  coefficients.

Our analysis has shown that the proposed wavefunction (Equation 2) is a valid solution for a periodic crystal. Let us first examine the implications of this solution. We can express the *Bloch wavefunction* as:

$$\psi_{\mathbf{k}}(\mathbf{r}) = \sum_{\mathbf{G}} C_{\mathbf{G}}(\mathbf{k}) e^{i(\mathbf{k}+\mathbf{G}) \cdot \mathbf{r}} = \left( \sum_{\mathbf{G}} C_{\mathbf{G}}(\mathbf{k}) e^{i\mathbf{G} \cdot \mathbf{r}} \right) e^{i\mathbf{k} \cdot \mathbf{r}} = u(\mathbf{r}) e^{i\mathbf{k} \cdot \mathbf{r}}$$

Note that  $u(\mathbf{r}) = \sum_{\mathbf{G}} C_{\mathbf{G}}(\mathbf{k}) e^{i\mathbf{G} \cdot \mathbf{r}}$  is a periodic function, since for any lattice translation vector  $\mathbf{T}$  it follows that  $u(\mathbf{r} + \mathbf{T}) = u(\mathbf{r})$ , after making use of the fact that  $\mathbf{G} \cdot \mathbf{T} = 2\pi n$  ( $n = \text{integer}$ ). This leads us to **Bloch's theorem** which states that the electron wavefunction in a crystal is simply a plane wave  $e^{i\mathbf{k} \cdot \mathbf{r}}$  multiplied by a periodic function. Note that a plane wave was also the solution for a free electron solid, where electron-nuclear interactions were ignored. This implies that Bloch electrons can travel freely through the crystal despite the presence of nuclei! Hence the mean free path  $\lambda$  can be larger than the atomic spacing<sup>1</sup>.

### **Bloch waves and Band structure**

Let us explore Equation 5 in more detail. There are an infinite number of reciprocal vectors  $\mathbf{G}$ , since by definition any periodic object is infinitely repeating, but in reality the potential  $V(\mathbf{r})$  will only depend on a finite number of reciprocal vectors, with the Fourier coefficients  $V_{\mathbf{G}}$  for higher order reciprocal vectors being zero. Assume that we need only  $N$  reciprocal vectors  $\mathbf{G}_1, \mathbf{G}_2, \dots, \mathbf{G}_N$  to represent  $V(\mathbf{r})$ . Equation 5 can then be written in matrix form:

$$\begin{pmatrix} \left( \frac{\hbar^2}{2m} |\mathbf{k} + \mathbf{G}_1|^2 - E \right) & \cdots & V_{\mathbf{G}_1 - \mathbf{G}_N} \\ \vdots & \ddots & \vdots \\ V_{\mathbf{G}_N - \mathbf{G}_1} & \cdots & \left( \frac{\hbar^2}{2m} |\mathbf{k} + \mathbf{G}_N|^2 - E \right) \end{pmatrix} \begin{Bmatrix} C_{\mathbf{G}_1} \\ \vdots \\ C_{\mathbf{G}_N} \end{Bmatrix} = \begin{Bmatrix} 0 \\ \vdots \\ 0 \end{Bmatrix} \quad \dots (6)$$

For non-trivial solutions of the  $C_{\mathbf{G}}$  coefficients the determinant of the square matrix must be zero:

$$\begin{vmatrix} \left( \frac{\hbar^2}{2m} |\mathbf{k} + \mathbf{G}_1|^2 - E \right) & \cdots & V_{\mathbf{G}_1 - \mathbf{G}_N} \\ \vdots & \ddots & \vdots \\ V_{\mathbf{G}_N - \mathbf{G}_1} & \cdots & \left( \frac{\hbar^2}{2m} |\mathbf{k} + \mathbf{G}_N|^2 - E \right) \end{vmatrix} = 0 \quad \dots (7)$$

---

<sup>1</sup> Strictly speaking  $\lambda$  should be infinite, but finite values are obtained in practice because thermal vibration of the atoms lead to small deviations from exact periodicity.

If we expand Equation 7 we obtain a  $N$ -order polynomial in the energy ( $E$ )<sup>2</sup>. This means that for a given wavevector  $\mathbf{k}$  there are  $N$  number of energies for the electron. This important result has a straightforward physical interpretation. In the free electron theory the electron energy has the form  $E \propto k^2$  and increases monotonically about the  $\mathbf{k} = 0$  point. However, because a crystal is periodic, and there is nothing to distinguish  $\mathbf{G}$  from  $\mathbf{k} = 0$ , we must create copies of the dispersion curve at each reciprocal point  $\mathbf{G}$  (Figure 1). Extrapolating these extra dispersion curves into the first Brillouin zone (i.e. the region between  $-\mathbf{G}/2$  and  $\mathbf{G}/2$ ) we obtain the additional electron energy values predicted by Equation 7.

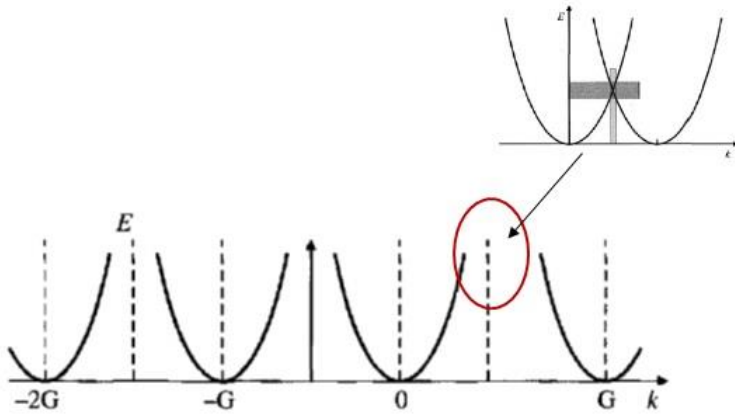


**Figure 1**

The energies do not always correspond to the free electron case; we have already seen from the nearly-free electron model that whenever electrons have similar energy (e.g. at the Brillouin zone boundary where two of the dispersion curves cross; Figure 1) there will be strong mixing between the electron states leading to non-degenerate energy levels.

There is a more useful way to think about the situation depicted in Figure 1. Consider the dispersion curve centred about  $\mathbf{k} = 0$  (Figure 2a). Overall the curve has the free electron form  $E \propto k^2$  except at the Brillouin zone boundaries, where strong mixing of states give rise to band gaps. This is called the **extended zone scheme**, since all  $\mathbf{k}$ -vectors are represented. However, for a crystal the periodicity means that the electron wavefunction is uniquely defined for  $\mathbf{k}$ -vectors within the first Brillouin zone, i.e. if  $\mathbf{k}'$  is a wavevector within the first Brillouin zone then  $\psi_{\mathbf{k}'}(\mathbf{r}) = \psi_{\mathbf{k}' + \mathbf{G}}(\mathbf{r})$  (note that the vector  $\mathbf{k}' + \mathbf{G}$  lies outside the first Brillouin zone). Therefore, the dispersion curve in the extended zone scheme can be folded back into the first Brillouin zone as shown in Figure 2b. This is known as the **reduced zone scheme** and is equivalent to Figure 1. The reduced zone scheme also predicts multiple electron energies for a given  $\mathbf{k}$ . The different branches of the electron energy represent the **band structure** of the solid. The number of available electronic states in a given band is equal to twice the number of primitive unit cells in the material (see previous lecture). Electrons will occupy the band with the lowest energy first, before moving onto the next band higher up in energy.

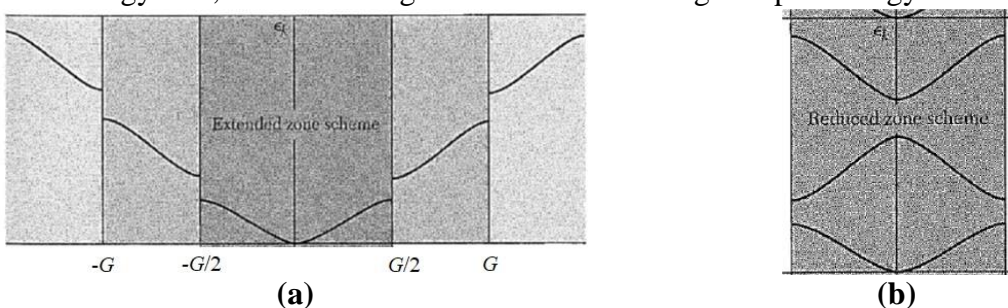


**Figure 2:** (a) Extended and (b) reduced zone schemes for the dispersion curve.

<sup>2</sup> If you have difficulty seeing how this comes about consider the simpler case where  $N = 2$ . The matrix elements are then as given in Equation 6 and the determinant in Equation 7 leads to a quadratic expression in  $E$ .

## FoP3B Part I Lecture 4: Effective mass and Introduction to Magnetism

### *Effective mass of electrons*

An important concept is the **effective mass** of electrons in a solid. A simple way to think about effective mass is as follows. Consider first an electron in free space. We apply a force  $F$  and measure the acceleration  $a$ . The mass can then be determined from  $F = ma$ . Now consider an electron in a real crystal subject to the same external force. As the electron moves through the crystal it will undergo Coulomb scattering with other electrons as well as atomic nuclei. The presence of these *internal* forces means that  $F \neq ma$  (recall that  $F$  is the *external* applied force). To satisfy Newton's second law we can therefore write  $F = m^*a$ , where  $m^*$  is the *effective* mass. It can be shown that for an isotropic crystal (see DUO supplementary material):

$$m^* = \frac{\hbar^2}{(d^2E/dk^2)}$$

where  $d^2E/dk^2$  is the curvature of electronic band (note that for anisotropic crystals we have to define an *effective mass tensor*  $m_{ij}^* = \hbar^2 / (dk_i dk_j)$ ).

### Introduction to Magnetism

#### *Magnetic dipole moment*

According to the Biort-Savart law moving charge (i.e. an electric current) generates a magnetic field. A special case is an electric current flowing in a loop (Figure 1).

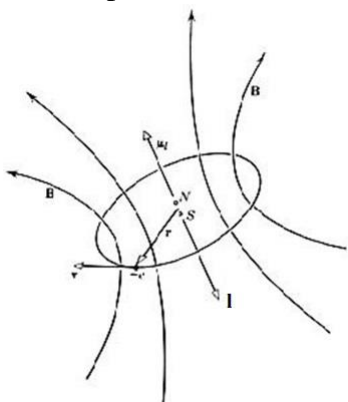


Figure 1

The magnetic field here is similar to that of a North-South pole bar magnet placed at the centre. We define a **magnetic dipole moment** to characterise the strength and orientation of the bar magnet. The magnetic moment  $\mu = IA$ , where  $I$  is the current (recall that current is defined as the flow of *positive* charge) and  $A$  is the *area vector* of the current loop, as defined by the right hand rule. The direction of  $\mu$  points from the South to North pole. Furthermore, for a negatively charged electron  $\mu$  is anti-parallel to the angular momentum  $\mathbf{l} = \mathbf{r} \times \mathbf{p}$ , where  $\mathbf{r}$  is the radial vector and  $\mathbf{p}$  is the linear momentum (Figure 1). Therefore, we may write  $\mu = -\gamma l$ , where  $\gamma$  is the **gyromagnetic ratio**.

It turns out that the magnetic moment for an electron has a fixed magnitude, called the **Bohr magneton**  $\mu_B$ , irrespective of the size of the circular orbit. It is therefore a fundamental unit for quantifying magnetic moments in solids. Consider an electron in a circular orbit of radius  $r$  at speed  $v$ . The time taken for the electron to do a circular loop is  $T = (2\pi r/v)$ . The current is  $I = e/T = ev/(2\pi r)$ , so that:

$$\mu_B = IA = \frac{ev}{2\pi r} \cdot \pi r^2 = \frac{e}{2m} (mv r)$$

The term  $mv r$  is the angular momentum. It therefore follows that  $\gamma = e/2m$ . The angular momentum can be calculated using some elementary quantum mechanics. The electron must

form a standing wave around the circular orbit, so that the circumference must be equal to an integer number of wavelengths  $\lambda$ , i.e.  $n\lambda = 2\pi r$ . Furthermore, by de Broglie's equation  $\lambda = \frac{h}{mv}$ , so that for the ground state ( $n=1$ ) we obtain  $mvr = \hbar$ , and consequently  $\mu_B = \gamma\hbar = \frac{e\hbar}{2m}$ . Note that this result is independent of the radius  $r$ . In fact  $\mu_B = 9.3 \times 10^{-24} \text{ Am}^2$ .

### **Some definitions and terminology**

Definitions and terminology in magnetism can sometimes be rather confusing. Here we will use SI units, rather than CGS units still used in some books! The equation for magnetic fields in vacuum is  $\mathbf{B} = \mu_0 \mathbf{H}$ , where  $\mathbf{H}$  is the magnetic field (units  $\text{Am}^{-1}$ ),  $\mu_0 = 4\pi \times 10^{-7} \text{ Hm}^{-1}$  (Henry per metre) is the permeability of free space and  $\mathbf{B}$  is the magnetic *induction* field (units Tesla, T)<sup>1</sup>. In vacuum  $\mathbf{B}$  and  $\mathbf{H}$  are simply proportional to one another, so that there is no significant difference between the two. However, in the interior of a magnetic solid we have  $\mathbf{B} = \mu_0(\mathbf{H} + \mathbf{M})$ , where  $\mathbf{M}$  is the *magnetisation* or net magnetic moment per unit volume (recall that the magnetic moment  $\mathbf{\mu}$  is a vector, so both the direction and magnitude must be taken into account when determining  $\mathbf{M}$ ).  $\mathbf{M}$  has the same units as  $\mathbf{H}$  (i.e.  $\text{Am}^{-1}$ ) and means  $\mathbf{B}$  is no longer proportional to  $\mathbf{H}$ .

The **magnetic susceptibility** is given by  $\chi = \mathbf{M}/\mathbf{H}$ .  $\chi$  is a dimensionless quantity and is defined for small values of  $\mathbf{H}$  where the *magnetisation curve* (i.e.  $M$  vs.  $H$  curve) shows linear behaviour<sup>2</sup>. From  $\mathbf{B} = \mu_0(\mathbf{H} + \mathbf{M})$  it is clear that if  $\chi < 0$  the  $\mathbf{B}$ -field will be smaller within the solid compared to vacuum, i.e. the material shows **diamagnetism** and repels magnetic fields. The opposite situation arises for  $\chi > 0$ . Typically, these would be materials showing weak magnetism (**paramagnetism**) or strong magnetism (**ferromagnetism**), although other forms of magnetic ordering are also possible as we shall see later in the course. The supplementary reading in DUO describes how we can measure the magnetic properties of materials using techniques such as vibrating sample magnetometry (VSM).

### **Magnetism as a quantum mechanical phenomenon**

The potential energy ( $E$ ) of a magnetic moment  $\mathbf{\mu}$  in a  $\mathbf{B}$ -field is  $E = -\mathbf{\mu} \cdot \mathbf{B}$ . The energy is therefore a minimum when  $\mathbf{\mu}$  is parallel to  $\mathbf{B}$ . Therefore, the magnetisation  $M = -\frac{dE_{\text{vol}}}{dB}$ , where  $E_{\text{vol}}$  is the energy per unit volume. Now because the Lorentz force  $\mathbf{F} = -e(\mathbf{v} \times \mathbf{B})$  is normal to the velocity  $\mathbf{v}$  a magnetic field cannot do any work on a moving electron. Therefore, according to classical physics the magnetisation must be zero! The response of a magnetic moment  $\mathbf{\mu}$  to a  $\mathbf{B}$ -field is illustrated in Figure 2.

---

<sup>1</sup> To further complicate matters  $\mathbf{H}$  is sometimes referred to as the magnetic field strength and  $\mathbf{B}$  the magnetic flux density.

<sup>2</sup> In certain strong magnetic materials, called ferromagnets (e.g. Fe, Co and Ni), the magnetisation graph is non-linear. The magnetic susceptibility is then defined as the gradient of the graph, i.e.  $\chi = d\mathbf{M}/d\mathbf{H}$  for small  $\mathbf{H}$ .

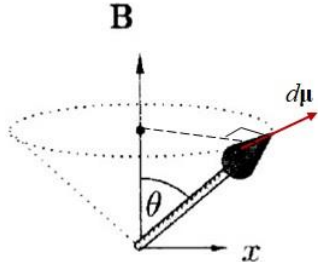


**Figure 2**

The torque  $\tau$  on the moment is  $\tau = \mu \times B$ . Since  $\tau = dI/dt$  (rate of change of angular momentum) and  $\mu = -\gamma I$ :

$$\frac{d\mu}{dt} = -\gamma(\mu \times B)$$

The change in moment  $d\mu$  is therefore perpendicular to  $\mu$ , so that the magnetic moment *precesses* around the  $B$ -field (Figure 2). Because the angle  $\theta$  between  $\mu$  and  $B$  does not change the potential energy is constant. Note that this behaviour is very different to electric dipoles, which do not have angular momentum and therefore *can* rotate under an applied electric field to minimise its energy.

The **Bohr-van Leeuwen theorem** states the above more rigorously: the magnetisation at thermal equilibrium for a solid obeying classical statistical mechanics (i.e. Maxwell-Boltzmann distribution) is zero. This is essentially due to the fact that the partition function for the electrons is not dependent on the magnetic field. The implication is that magnetism is Quantum Mechanical in origin.

## FoP3B Part I Lecture 5: Diamagnetism

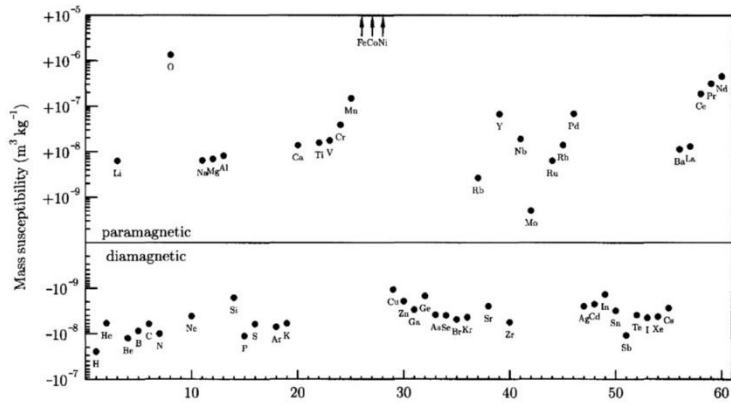


**Figure 1**

Figure 1 shows the mass susceptibility (i.e. magnetic susceptibility divided by the material density) for various elements in the periodic table. The majority of elements are either weakly magnetic (i.e. paramagnetic with  $\chi > 0$ ) or diamagnetic ( $\chi < 0$ )<sup>1</sup>. In this lecture we will explore diamagnetism, using both classical and quantum physics.

### Langevin's theory of diamagnetism

The classical theory of diamagnetism is due to Paul Langevin. Consider the precession of a magnetic moment  $\mu$  in a  $\mathbf{B}$ -field applied along the  $z$ -axis (Figure 2).

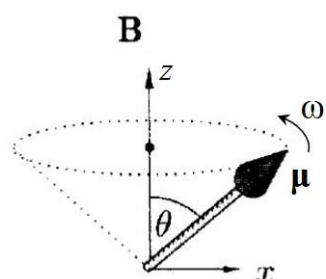


**Figure 2**

From the precession formula  $\frac{d\mu}{dt} = -\gamma(\mu \times \mathbf{B})$ :

$$\frac{d\mu_x}{dt} = -\gamma B \mu_y ; \frac{d\mu_y}{dt} = \gamma B \mu_x \text{ and } \frac{d\mu_z}{dt} = 0$$

The fact that the  $z$ -component of  $\mu$  is unchanged with time is indicative of precessional motion. If at time  $t = 0$  the moment  $\mu$  is in the  $xz$ -plane, the above differential equations give:

$$\mu_x(t) = \mu \sin \theta \cos(\omega t) ; \mu_y(t) = \mu \sin \theta \sin(\omega t)$$

Here the angular frequency  $\omega = \gamma B = \frac{eB}{2m}$  is known as the **Larmor precession frequency**. We saw in the previous lecture that electrons in a circular orbit generate magnetic moments. In the presence of a magnetic field, in addition to the circular motion, there will also be Larmor precessional motion which generates its own magnetic moment. From Figure 2 it is clear that the precessional moment is anti-parallel to the  $\mathbf{B}$ -field (recall that we define current as the flow of *positive* charge, while electrons are negatively charged). Therefore, there is a magnetic field generated by precession that *opposes* the external field. This is the origin of diamagnetism according to classical physics. In some cases, this is described as being similar to **Lenz's law** from the theory of electromagnetic induction, although this is misleading, since Lenz's law only applies to time-dependent magnetic fields, whereas in our case the  $\mathbf{B}$ -field can be static.

Let us calculate the magnitude of the precessional magnetic moment. The precession period is  $T = 2\pi/\omega = 4\pi m/eB$  and the precession current is  $I = e/T = e^2 B / 4\pi m$ . To calculate the induced moment we need to multiply  $-I$  by the area of current loop, i.e.  $\pi \langle \rho^2 \rangle$ , where  $\langle \rho^2 \rangle$  is the mean square radius of the precessing electron from the atom nucleus. Note the minus sign in  $-I$  is to

<sup>1</sup> In fact, it is a misconception that magnetism is a rare phenomenon!

indicate that the induced moment opposes the applied **B**-field. For a spherically symmetric atom  $\langle x^2 \rangle = \langle y^2 \rangle = \langle z^2 \rangle$  (i.e. we cannot distinguish between x,y and z-directions). Since  $\langle r^2 \rangle = \langle x^2 \rangle + \langle y^2 \rangle + \langle z^2 \rangle$ , we have  $\langle \rho^2 \rangle = \langle x^2 \rangle + \langle y^2 \rangle = 2/3 \langle r^2 \rangle$ . The magnetic moment of a single electron is  $-I(\pi \langle \rho^2 \rangle)$  or  $-e^2 B \langle r^2 \rangle / 6m$ . Assume there are  $n$  atoms/ions per unit volume each with  $Z$  electrons. The magnetisation  $M$  is therefore:

$$M = -\frac{ne^2 Z B \langle r^2 \rangle}{6m}$$

For weak magnetisation  $\mathbf{B} = \mu_0(\mathbf{H}+\mathbf{M}) \approx \mu_0\mathbf{H}$ . Therefore  $\chi = M/H = \mu_0 M/B$ . The diamagnetic susceptibility is then:

$$\chi = -\frac{ne^2 \mu_0 Z \langle r^2 \rangle}{6m}$$

Note that the diamagnetic susceptibility is independent of temperature.

Although it may appear that diamagnetism is compatible with classical physics, we still have to keep in mind the Bohr-van Leeuwen theorem, which states that the equilibrium magnetisation is zero for a classical system. Figure 3 shows how we might reconcile these two seemingly conflicting results; the Larmor precession orbits of all the internal electrons within the solid reinforce one another, such that their net effect can be represented by a larger orbit taken in the same sense (i.e. anti-clockwise) along the surface boundary of the solid.

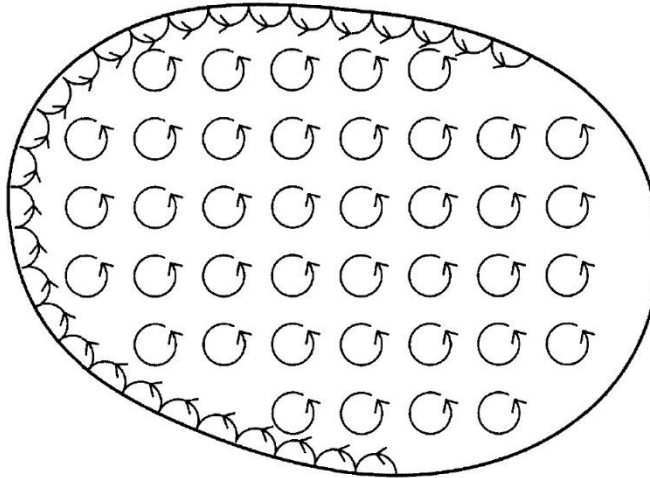


**Figure 3**

However, those electrons that are close to the surface can complete only half of the Larmor precession orbit (known as *skipping orbits*), and *overall* these run in the opposite sense (i.e. clockwise) to the internal electron orbits. The induced magnetic moment from the internal electrons are therefore cancelled by the surface electrons, giving a zero net magnetisation as required. We must therefore look to quantum mechanics to find the exact origin of diamagnetism.

### **Quantum Mechanical Treatment**

We start by considering the Hamiltonian for a single electron in a magnetic field **B**:

$$\hat{H} = \frac{(\mathbf{p} + e\mathbf{A})^2}{2m} + V + g_s \gamma \mathbf{B} \cdot \mathbf{s}$$

The first term is the kinetic energy with the momentum **p** replaced by the canonical momentum  $(\mathbf{p}+e\mathbf{A})$ , where  $\mathbf{B} = \nabla \times \mathbf{A}$  and  $\mathbf{A}$  is the magnetic vector potential. The canonical momentum is due to the Lorentz force acting on the electron; its derivation can be found in the Supplementary Reading on DUO. The second term in the Hamiltonian is the standard potential energy  $V$ . The final term is the energy due to the electron spin angular momentum  $\mathbf{s}$ ; this has the form of

energy of a magnetic moment  $\mu$  in an applied field, i.e.  $-\mu \cdot \mathbf{B} = \gamma \mathbf{B} \cdot \mathbf{l}$ , with  $\mathbf{s}$  replacing the angular momentum  $\mathbf{l}$ . The term  $g_s$  is the Landé g-factor and has a value that is very nearly 2.

If we set the gauge as  $\mathbf{A}(\mathbf{r}) = (\mathbf{B} \times \mathbf{r})/2$ , then:

$$\hat{H} = \left( \frac{\mathbf{p}^2}{2m} + V \right) + \frac{e}{m} (\mathbf{p} \cdot \mathbf{A}) + g_s \gamma \mathbf{B} \cdot \mathbf{s} + \frac{e^2 \mathbf{A}^2}{2m}$$

But <sup>2</sup>  $\frac{e}{m} (\mathbf{p} \cdot \mathbf{A}) = \frac{e}{2m} \mathbf{p} \cdot (\mathbf{B} \times \mathbf{r}) = \gamma \mathbf{B} \cdot (\mathbf{r} \times \mathbf{p})$  and  $\mathbf{l} = \mathbf{r} \times \mathbf{p}$ , so that:

$$\hat{H} = \left( \frac{\mathbf{p}^2}{2m} + V \right) + \gamma \mathbf{B} \cdot (\mathbf{l} + g_s \mathbf{s}) + \frac{e^2}{8m} (\mathbf{B} \times \mathbf{r})^2$$

The second and third terms represent the magnetic contribution to the standard Hamiltonian. They are known as the paramagnetic and diamagnetic terms respectively. Let us examine the latter in more detail. By first order perturbation theory the energy change ( $\Delta E$ ) to the ground state wavefunction  $|0\rangle$  due to the diamagnetic term is (see Lecture 2):

$$\Delta E = \frac{e^2}{8m} \langle 0 | (\mathbf{B} \times \mathbf{r})^2 | 0 \rangle$$

If  $\mathbf{B}$  is along the  $z$ -axis then  $(\mathbf{B} \times \mathbf{r})^2 = B^2(x^2+y^2)$ . Therefore:

$$\Delta E = \frac{e^2 B^2}{8m} \{ \langle 0 | x^2 | 0 \rangle + \langle 0 | y^2 | 0 \rangle \}$$

The first and second terms within the curly brackets are the expectation values for  $x^2$  and  $y^2$  respectively, i.e.  $\langle x^2 \rangle, \langle y^2 \rangle$ . Since  $\langle x^2 \rangle = \langle y^2 \rangle = \langle r^2 \rangle / 3$  for electrons in spherical atoms:

$$\Delta E = \frac{e^2 B^2}{12m} \langle r^2 \rangle$$

Note that the energy change  $\Delta E$  is always positive. Hence the diamagnetic term will always repel the applied  $\mathbf{B}$ -field in order to lower the energy of the solid. The magnetic moment  $\mu = -d(\Delta E)/dB$ , so that for  $n$  atoms/ions per unit volume each with  $Z$  electrons the magnetisation is  $M = -\frac{ne^2 Z B}{6m} \langle r^2 \rangle$ . For weak magnetisation (i.e.  $\chi = \mu_0 M/B$ ):

$$\chi = -\frac{ne^2 \mu_0 Z \langle r^2 \rangle}{6m}$$

Fortuitously, this is the same result as derived from Langevin theory! However, the origins are rather different. Diamagnetism is due to a  $\frac{e^2}{8m} (\mathbf{B} \times \mathbf{r})^2$  term in the Hamiltonian, which is present in every solid. In some solids the paramagnetic term  $\gamma \mathbf{B} \cdot (\mathbf{l} + g_s \mathbf{s})$  may be larger, thereby giving rise to net paramagnetic behaviour, although the weaker diamagnetic contribution will still be present.

---

<sup>2</sup> We use the cyclic permutation property of the scalar product between three vectors  $\mathbf{a}, \mathbf{b}$  and  $\mathbf{c}$ , i.e.  $\mathbf{a} \cdot (\mathbf{b} \times \mathbf{c}) = \mathbf{b} \cdot (\mathbf{c} \times \mathbf{a}) = \mathbf{c} \cdot (\mathbf{a} \times \mathbf{b})$ .

### **Delocalised electrons and magnetic anisotropy**

An interesting situation arises for materials, such as a benzene molecule or graphite, that contain so-called *delocalised electrons*. Taking benzene ( $C_6H_6$ ) as an example we have a hexagonal arrangement of carbon atoms with each carbon atom bonded to a hydrogen atom (Figure 4). For a stable electronic configuration carbon has to form four covalent bonds. This can be achieved by carbon forming a double bond with either one of its neighbouring carbon atoms. There are therefore two possible structural configurations; however, quantum mechanics predicts that the electron will be delocalised, rather than being confined to a single double bond. The delocalised electron, also known as  $\pi$ -electrons, spreads over the entire molecule (Figure 4), so that its radius  $\langle r \rangle$  is now the size of the molecule, rather than a single atom. Since the susceptibility depends on  $\langle r^2 \rangle$  compounds such as benzene and graphite show strong diamagnetic behaviour.

There is also a subtlety arising from the fact that the diamagnetism is ultimately due to the  $\frac{e^2}{8m}(\mathbf{B} \times \mathbf{r})^2$  Hamiltonian term. If the  $\mathbf{B}$ -field is applied parallel to the benzene molecule or graphite planes then  $\mathbf{B} \times \mathbf{r} = \mathbf{0}$ , so that the susceptibility  $\chi$  along this direction is zero. The absolute value of  $\chi$  will however be a maximum for  $\mathbf{B}$ -fields that are normal to the benzene molecule or graphite planes. This phenomenon, where the magnetic response depends on the direction of the applied  $\mathbf{B}$ -field is known as **magnetic anisotropy**.

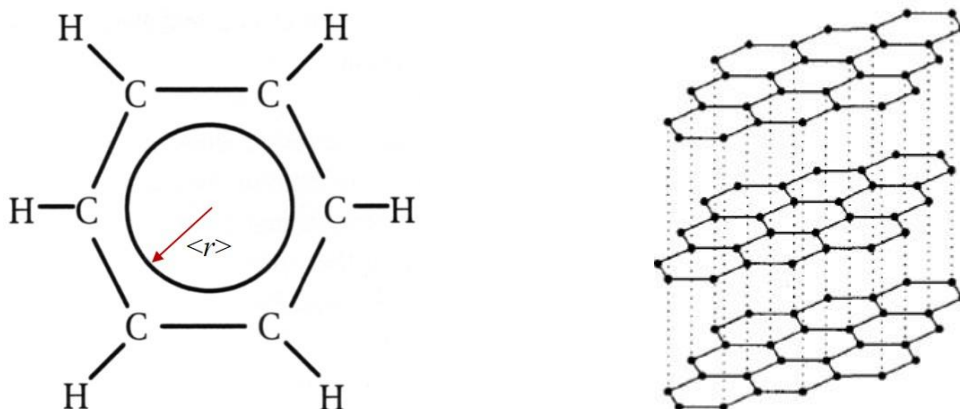


**Figure 4:** A benzene molecule (left) and graphite solid (right)

## FoP3B Part I Lecture 6: Multi-electron atoms and Hund's rules

The magnetic moment  $\mu$  and angular momentum are related by  $\mu = -\gamma \mathbf{l}$ . At the same time the Bohr-van Leeuwen theorem predicts zero magnetisation for electrons obeying classical statistical physics. This hints that angular momentum in quantum mechanics behaves rather differently to the classical world. In this lecture we will explore electron angular momentum in multi-electron atoms using quantum mechanics, and show how it leads to magnetism in solids.

### Quantum Mechanical Angular Momentum

From  $\mathbf{l} = \mathbf{r} \times \mathbf{p}$  the **orbital angular momentum** operator is defined as  $\hat{\mathbf{l}} = \mathbf{r} \times (-i\hbar\vec{\nabla}) = -i\hbar\mathbf{r} \times \vec{\nabla}$ . It can be shown that:

$$\begin{aligned} [\hat{l}_x, \hat{l}_y] &= i\hbar\hat{l}_z \\ [\hat{l}_y, \hat{l}_z] &= i\hbar\hat{l}_x \\ [\hat{l}_z, \hat{l}_x] &= i\hbar\hat{l}_y \end{aligned}$$

The square brackets represent the commutator<sup>1</sup>. In quantum mechanics any two operators with zero commutator represent *compatible measurements*, i.e. the two operators share a common electron wavefunction, so that the properties represented by the two operators can both be measured simultaneously with no error. From the above it is clear that no two components of the orbital angular momentum can be known simultaneously. However,  $[\hat{l}^2, \hat{l}_x] = [\hat{l}^2, \hat{l}_y] = [\hat{l}^2, \hat{l}_z] = 0$ , i.e. it is possible to know both the magnitude and only *one* component (say the  $z$ -component) of  $\mathbf{l}$ .

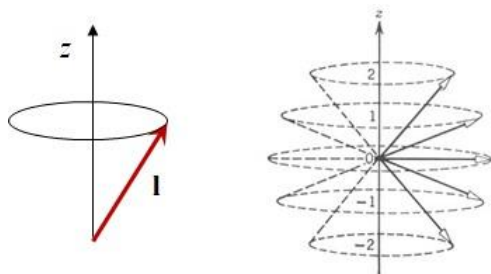


**Figure 1**

Figure 1 (left) illustrates the situation; the length of the vector  $\mathbf{l}$  and its projection along  $z$  are known. The vector  $\mathbf{l}$  precesses about the  $z$ -axis, consistent with the fact that the  $x, y$  components are unknown.

Furthermore, we have the following relationships:

$$\begin{aligned} |\mathbf{l}| &= \sqrt{l(l+1)}\hbar \\ l_z &= m_l\hbar \\ m_l &= l, l-1, \dots, 0, -1, \dots, -l \end{aligned}$$

$l$  and  $m_l$  are quantum numbers that can take only integer values. The former determines the magnitude of  $\mathbf{l}$ , while the latter determines the  $z$ -component. An example for  $l = 2$  is shown in Figure 1 (right). Note that vector magnitude is constant, but its orientation changes depending on the  $m_l$  value. For  $l = 2$  there are only five orientations (w.r.t.  $z$ -axis); this behaviour is very different to classical angular momentum which is a continuous variable.

The magnetic moment due to orbital angular momentum is  $\mu_l = -\gamma \mathbf{l}$  so that  $\mu_{lz} = -\gamma l_z = -(\gamma\hbar)m_l = -\mu_B m_l$ . The energy in a magnetic field is therefore  $E = -\mu_l \cdot \mathbf{B} = \mu_B B m_l$ .

---

<sup>1</sup> For any two operators A and B  $[A, B] = AB - BA$ . Operators with non-zero commutator cannot be measured simultaneously, e.g. position and momentum in Heisenberg's uncertainty principle.

Apart from orbital angular momentum electrons also possess an intrinsic **spin angular momentum**,  $\mathbf{s}$ , that has no classical equivalent<sup>2</sup>. The quantum mechanical conditions for  $\mathbf{s}$  are similar to  $\mathbf{l}$ :

$$|\mathbf{s}| = \sqrt{s(s+1)}\hbar \quad (s = \frac{1}{2})$$

$$s_z = m_s\hbar$$

$$m_s = s, s-1 = \frac{1}{2}, -\frac{1}{2}$$

Note that the spin quantum number  $s$  can only take the value of  $\frac{1}{2}$ , so that there are only two values for  $m_s$ , i.e.  $+\frac{1}{2}, -\frac{1}{2}$ , corresponding to spin up and spin down electrons. The magnetic moment due to spin angular momentum is  $\boldsymbol{\mu}_s = -\gamma g_s \mathbf{s}$ , where  $g_s$  is the Landé  $g$ -factor ( $g_s \approx 2$ ).

The orbital and spin angular momentum can couple in what is called **spin-orbit interaction**. This is illustrated in Figure 2.

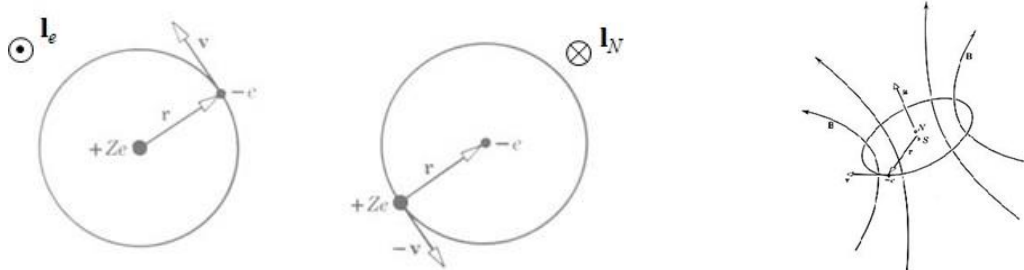


**Figure 2:** electron orbiting the nucleus (left) and the same situation as viewed from the electron frame of reference (middle) resulting in an internal  $\mathbf{B}$ -field (right)

The electron orbits the nucleus, but when viewed from its own frame of reference the electron sees the nucleus orbiting around it. The nuclear orbital angular momentum  $\mathbf{l}_N$  is anti-parallel to that of the electron  $\mathbf{l}_e$ . There will be a magnetic moment,  $\boldsymbol{\mu}_N = -\gamma \mathbf{l}_N$ , associated with  $\mathbf{l}_N$ , which generates a strong *internal* magnetic  $\mathbf{B}$ -field that is parallel to  $\mathbf{l}_e$ . The electron spin angular momentum  $\mathbf{s}$  therefore has a potential energy  $\Delta E = -\boldsymbol{\mu}_s \cdot \mathbf{B}$  due to the internal  $\mathbf{B}$ -field arising from the orbital angular momentum. It can be shown that the spin-orbit interaction energy:

$$\Delta E = \frac{1}{2mc^2r} \frac{dV(r)}{dr} \mathbf{s} \cdot \mathbf{l}$$

where  $V(r)$  is the potential due to the atomic nucleus and  $c$  is the speed of light. The spin-orbit interaction is greater for heavy atoms with large  $V(r)$ . Since the  $\mathbf{B}$ -field causing spin-orbit interaction is internal, there are no external torques, meaning that angular momentum is conserved and  $\mathbf{j} = \mathbf{l} + \mathbf{s}$ . The quantum rules for angular momentum  $\mathbf{j}$  are:

$$|\mathbf{j}| = \sqrt{j(j+1)}\hbar ; \quad j = l+s, |l-s| \\ j_z = m_j\hbar ; \quad m_j = j, j-1, \dots, -j$$

<sup>2</sup> Spin arises from relativistic quantum mechanics, i.e. Dirac's theory of the electron.

Note that these rules are similar for  $\mathbf{l}$  and  $\mathbf{s}$  apart from the values for the  $j$  quantum number<sup>3</sup>.

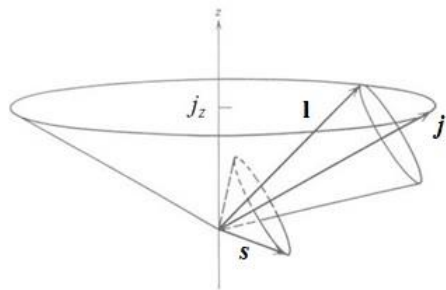


**Figure 3**

The spin-orbit interaction is illustrated in Figure 3:  $\mathbf{l}$  and  $\mathbf{s}$  precess together about  $\mathbf{j}$  due to torques induced by the internal  $\mathbf{B}$ -field.  $\mathbf{j}$  can lie anywhere on the cone with constant  $j_z$ . Note that  $m_l$  and  $m_s$  are no longer good quantum numbers, i.e. the  $z$ -components of  $\mathbf{l}$  and  $\mathbf{s}$  are not known after spin-orbit coupling.

Consider now the spin-orbit interaction energy  $\Delta E$  which depends on  $\mathbf{s} \cdot \mathbf{l}$ . From  $\mathbf{j} = \mathbf{l} + \mathbf{s}$ ,

$$|\mathbf{j}|^2 = |\mathbf{l}|^2 + |\mathbf{s}|^2 + 2\mathbf{s} \cdot \mathbf{l}$$

Or  $j(j+1)\hbar = l(l+1)\hbar + s(s+1)\hbar + 2\mathbf{s} \cdot \mathbf{l}$  which gives:

$$\mathbf{s} \cdot \mathbf{l} = \frac{\hbar}{2}[j(j+1) - l(l+1) - s(s+1)]$$

The Spin-orbit energy is therefore expected to increase with  $j$ . Spin-orbit energies are of the order  $10^{-4}$  eV for light atoms (i.e. much smaller than the few eV spacing between energy levels in an atom).

### Multi-electron atoms and Hund's rules

The electron configuration in a multi-electron atom must be such that the energy is minimised. The energy is due to: (i) Coulomb interaction and (ii) spin-orbit interaction. For light atoms the former is dominant and must be minimised first. This is known as **LS or Russel-Saunders coupling**. Coulomb energy has contributions from both spin and orbital angular momentum. Parallel spins are favoured (Figure 4a), since from the Pauli exclusion principle these are spaced far apart, thereby reducing the Coulomb energy. Hence the total spin angular momentum  $\mathbf{S} = \mathbf{s}_1 + \mathbf{s}_2 + \dots$  must be maximised, where  $\mathbf{s}_1, \mathbf{s}_2$ , are the spin angular momenta of the individual electrons. Similarly, the total orbital angular momentum  $\mathbf{L} = \mathbf{l}_1 + \mathbf{l}_2 + \dots$  must also be maximised; in Figure 4b if the two electrons both move in the same sense (i.e. clockwise or counter-clockwise) around the loop they stay far apart, whereas if they move in opposite senses they cross paths, thereby increasing the Coulomb energy. The  $\mathbf{S}$  and  $\mathbf{L}$  angular momenta can spin-orbit couple to give a new angular momentum  $\mathbf{J} = \mathbf{L} + \mathbf{S}$ .

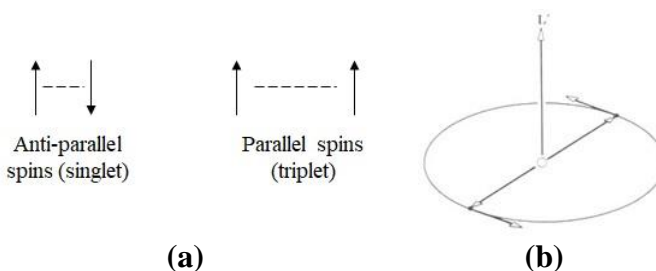


**Figure 4:** (a) distance between parallel and anti-parallel spins and (b) two electrons in a circular orbit. Coulomb energy is minimised for parallel spins in (a) and electrons orbiting in the same sense in (b).

<sup>3</sup> The rules for adding any two angular momenta  $\mathbf{q}$  and  $\mathbf{r}$  are as follows (note that  $\mathbf{q}, \mathbf{r}$  could represent two orbital or two spin momenta or alternatively one each of orbital and spin momenta): the  $z$ -component of  $\mathbf{p} = \mathbf{q} + \mathbf{r}$  is conserved, i.e.  $p_z = q_z + r_z$ . Since  $|\mathbf{p}| = \sqrt{p(p+1)}\hbar$  and  $p_z = m_p\hbar$  ( $m_p = p, p-1, \dots, -p$ ) and similarly for  $\mathbf{q}$  and  $\mathbf{r}$  this means that the maximum value for  $p$  is  $(q+r)$ .  $p$  can therefore take values  $q+r, q+r-1, q+r-2, \dots$  etc. The terminating point for the series is determined by the vector inequality  $|\mathbf{q}+\mathbf{r}| \geq \|\mathbf{q}\| - \|\mathbf{r}\|$ , which gives a minimum value for  $p$  of  $|q-r|$ . For  $\mathbf{j} = \mathbf{l} + \mathbf{s}$  there are thus only two values for  $j$  (i.e.  $l+s$  and  $|l-s|$ ) because  $s = 1/2$ .

**Hund's rules** govern the minimum energy electron configuration in atoms where  $LS$  coupling is present. The procedure for determining the electron configuration is as follows: (i) First maximise  $\mathbf{S}$ , (ii) next maximise  $\mathbf{L}$ , followed by (iii) selecting  $\mathbf{J}$  that gives the smallest spin-orbit interaction energy (this is  $J = |L - S|$  if the band is less than half-full and  $J = L + S$  for a band more than half-full<sup>4</sup>). Note that the larger Coulomb energy is minimised first before minimising the smaller spin-orbit interaction energy.

$m_l$	$m_s = \frac{1}{2}$	$m_s = -\frac{1}{2}$
3	•	•
2	•	•
1	•	
0	•	
-1	•	
-2	•	
-3	•	

**Figure 5**

As an example Figure 5 shows Hund's rules applied to a  $Dy^{3+}$  ion with a  $4f^9$  shell (NB:  $l=3$  for a  $f$ -shell)<sup>5</sup>. It can be seen that  $L = \sum m_l = 5$  and  $S = \sum m_s = 5/2$ . Strictly speaking,  $\sum m_l = m_L$ , where  $L_z = m_L \hbar$  and  $m_L$  can take any value of  $L, L-1, \dots, -L$ . However, since  $\mathbf{L}$  is maximised by Hund's rules we must have  $m_L = L$  and therefore  $L = \sum m_l$ . Similar arguments apply to  $S = \sum m_s$ .

Since the band is more than half-full  $J = L + S = 15/2$ . The electronic configuration is denoted by  $^{2S+1}L_J$ . ( $2S + 1$ ) is the spin multiplicity.  $L$  is denoted using the relevant letter from the table below:

L	0	1	2	3	4	5	6
	S	P	D	F	G	H	I

The electronic configuration of  $Dy^{3+}$  is therefore  $^6H_{15/2}$ . This is also known as the **term symbol**.

### Magnetism in multi-electron atoms

The magnetic Hamiltonian terms for a multi-electron atom is:

$$\sum_i \gamma \mathbf{B} \cdot (\mathbf{l}_i + g_s \mathbf{s}_i) + \begin{pmatrix} \text{spin - orbit} \\ \text{interaction} \end{pmatrix} + \frac{e^2}{8m} (\mathbf{B} \times \mathbf{r}_i)^2$$

For an atom with  $LS$  coupling:

$$\sum_i \gamma \mathbf{B} \cdot (\mathbf{l}_i + g_s \mathbf{s}_i) + \begin{pmatrix} \text{spin - orbit} \\ \text{interaction} \end{pmatrix} = \gamma \mathbf{B} \cdot (\mathbf{L} + g_s \mathbf{S}) + \begin{pmatrix} \text{spin - orbit} \\ \text{interaction} \end{pmatrix} = \gamma g_J \mathbf{B} \cdot \mathbf{J}$$

where  $g_J$  is a Landé  $g$ -factor for  $J$ :  $g_J = \frac{3}{2} + \frac{S(S+1)-L(L+1)}{2J(J+1)}$ . For a full shell  $\mathbf{L}$ ,  $\mathbf{S}$  and  $\mathbf{J} = 0$ , so that only the diamagnetic term remains (i.e. atoms/ions with filled shells show diamagnetic behaviour). On the other hand, for an incomplete shell  $\mathbf{L}$ ,  $\mathbf{S}$  and  $\mathbf{J} \neq 0$ , so that there will also be a paramagnetic contribution.

<sup>4</sup> We showed earlier that the spin-orbit interaction should generally increase with  $J$ . The minimum value of  $J$  is  $|L-S|$ , so we expect Hund's rules to always favour  $J = |L-S|$ . However, this condition only holds when the band is less than half-full.

<sup>5</sup> Hund's rules are typically always satisfied in Lanthanide ions, since the  $4f$  shell is screened from the rest of the solid by the  $5s$  and  $5p$  shells. In 3d transition metal ions the screening is not as strong, so that Hund's rules may break down in transition metal solids. In these solids a phenomenon known as 'orbital quenching' occurs where the favoured value of  $L$  is  $L = 0$ .

## FoP3B Part I Lecture 7: Paramagnetism

As seen previously most elements in the periodic table are either diamagnetic or paramagnetic, i.e. weakly magnetic. A paramagnetic solid is characterised by no *long range order* of the magnetic moments, so that the overall magnetisation is zero in the absence of an external **B**-field. Here we will explore paramagnetism using both classical and quantum physics.

### *Langevin theory of paramagnetism*

The classical theory of paramagnetism is due to Paul Langevin. Since there is no long range order we assume that the magnetic moments are randomly oriented in space and can lie anywhere on a unit sphere (Figure 1). If the **B**-field is along the *z*-axis magnetic moments with angles between  $\theta$  and  $\theta + d\theta$  to the applied field will cover an area  $(2\pi \sin \theta) d\theta$  on the unit sphere. The energy of a magnetic moment  $\mu$  is  $E = -\mu \cdot \mathbf{B} = -\mu B \cos \theta$ . Furthermore, since the magnetic moments are independent of one another, a fact that is consistent with the lack of any long range order, classical Maxwell-Boltzmann statistics should apply. The probability of a magnetic moment at angle  $\theta$  to the applied field is therefore proportional to  $\exp(-E/kT) = \exp(\mu B \cos \theta / kT)$ . The average moment  $\langle \mu_z \rangle$  is:

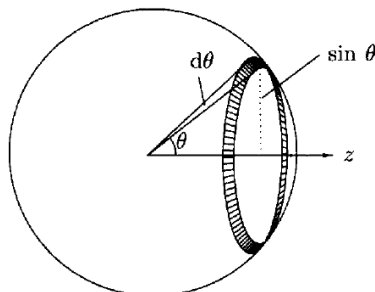


**Figure 1**

$$\langle \mu_z \rangle = \frac{\int_0^\pi (\mu \cos \theta) e^{\frac{\mu B \cos \theta}{kT}} (2\pi \sin \theta) d\theta}{\int_0^\pi e^{\frac{\mu B \cos \theta}{kT}} (2\pi \sin \theta) d\theta} = \mu \frac{\int_{-1}^1 x e^{yx} dx}{\int_{-1}^1 e^{yx} dx}$$

where  $y = \mu B / kT$  and  $x = \cos \theta$ . Hence

$$\frac{\langle \mu_z \rangle}{\mu} = \coth y - \frac{1}{y} = L(y)$$

$L(y)$  is called the **Langevin function**.

For determining magnetic susceptibility ( $\chi$ ), we are interested in weak magnetic fields, so that  $y \rightarrow 0$  and  $\lim_{y \rightarrow 0} \coth y = \frac{y}{3} + \frac{1}{y}$ . Therefore,  $\frac{\langle \mu_z \rangle}{\mu} = \frac{y}{3} = \frac{\mu B}{3kT}$ . For  $n$  moments per unit volume the magnetisation  $M = n\langle \mu_z \rangle$  and the *saturation* magnetisation  $M_s = n\mu$  (the saturation magnetisation is the largest magnetisation possible and occurs when all magnetic moments are parallel to the **B**-field). It follows that  $\frac{M}{M_s} = \frac{\langle \mu_z \rangle}{\mu} = \frac{\mu B}{3kT}$ . Furthermore, for a weak magnetic material  $B = \mu_0(H+M) \approx \mu_0 H$ , and  $\chi = M/H = \mu_0 M/B$ . We therefore finally obtain:

$$\chi = \frac{n\mu_0\mu^2}{3kT}$$

Note that the paramagnetic susceptibility is temperature dependent, unlike diamagnetic susceptibility. The  $\chi \propto 1/T$  dependence is known as **Curie's law**.

### *Quantum Mechanical theory of paramagnetism*

The quantum mechanical analysis of paramagnetism is similar to the Langevin theory, with the key difference being that the angular momentum component along the *z*-axis, and therefore its

associated magnetic moment, is a discrete, rather than continuous, variable. For an atom with  $LS$  coupling the paramagnetic Hamiltonian term is  $\gamma g_J \mathbf{B} \cdot \mathbf{J}$ . We will first consider the simplest case of atoms where  $L = 0$ ,  $S = 1/2$  and  $J = L + S = 1/2$  (e.g. a hydrogen atom). The  $J_z$  component is  $m_J \hbar$ , where  $m_J = 1/2, -1/2$ . Therefore,  $\mu_z = -g_J \gamma J_z$  and  $g_J = \frac{3}{2} + \frac{S(S+1)-L(L+1)}{2J(J+1)} = 2$ .  $\mu_z$  values are therefore  $\pm \gamma \hbar$  or  $\pm \mu_B$ . The average magnetic moment is:

$$\langle \mu_z \rangle = \frac{-\mu_B e^{\frac{\mu_B B}{kT}} + \mu_B e^{-\frac{\mu_B B}{kT}}}{e^{\frac{\mu_B B}{kT}} + e^{-\frac{\mu_B B}{kT}}} = \mu_B \tanh\left(\frac{\mu_B B}{kT}\right)$$

The exponential terms in the above Equation are the Maxwell-Boltzmann probabilities of finding a magnetic moment with energy  $\pm \mu_B B$ . Again assuming small  $\mathbf{B}$ -fields and using the fact that  $\tanh(y) \approx y$  for small values of  $y$ , gives  $\frac{M}{M_s} = \frac{\langle \mu_z \rangle}{\mu_B} = \frac{\mu_B B}{kT}$ . From  $\chi = \mu_0 M/B$  we get:

$$\chi = \frac{n \mu_0 \mu^2}{kT}$$

The susceptibility for a  $J = 1/2$  solid is therefore very similar to the Langevin result apart from a missing factor ‘3’ in the denominator. We can also calculate  $\chi$  for other (i.e. larger) values of  $J$  using a similar procedure, but because  $m_J = J, J-1, \dots, -J$  can now take many more values we need to consider the additional  $\mu_z$  contributions to  $\langle \mu_z \rangle$ .

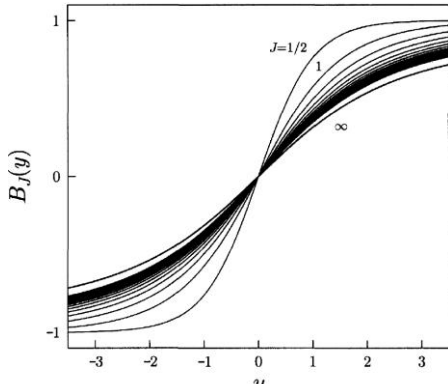


**Figure 2**

It is easy to show that:

$$\frac{M}{M_s} = B_J(y) \quad ; \quad y = \frac{g_J \mu_B J B}{kT}$$

where  $B_J(y)$  is the **Brillouin function**:

$$B_J(y) = \frac{2J+1}{2J} \coth\left(\frac{2J+1}{2J}y\right) - \frac{1}{2J} \coth\left(\frac{y}{2J}\right)$$

The Brillouin function is plotted in Figure 2 for all allowed values of  $J$  from  $J = 1/2$  to  $\infty$  (the latter corresponds to the Langevin case where magnetic moment is a continuous variable; in fact  $B_J(y) \rightarrow L(y)$  for  $J \rightarrow \infty$  giving the same result as Langevin theory).

### *Thermodynamic properties of paramagnetism and adiabatic cooling*

Using the results for a  $J = 1/2$  solid as an example we can calculate the thermodynamic properties of a paramagnet. Figure 3a shows the magnetisation  $M$  as a function of  $(kT/\mu_B B)$ ; it shows that as the temperature is decreased for a given  $\mathbf{B}$ -field, or alternatively magnetic field increased at constant temperature, the magnetisation gradually increases towards the saturation value  $M_s$ . This is because low temperature and strong  $\mathbf{B}$ -fields both favour alignment of the magnetic moments. The energy of the solid  $E = -MB$  is simply a mirror reflection of the magnetisation curve (Figure 3b). From the energy we can calculate the specific heat, using the relation  $C = \left(\frac{\partial E}{\partial T}\right)_B$ , as shown in Figure 3c. The specific heat shows a maximum, known as the **Schottky anomaly**. Its interpretation is straightforward: to the right of the maximum the magnetic moments are misaligned by thermal effects. At high enough temperature the moments are as

disordered as they can be, so that increasing the temperature further will not make any significant difference and the heat capacity will approach zero. To the left of the Schottky anomaly the moments become more aligned with decreasing temperature, until perfect order is reached and the heat capacity approaches zero. Finally, from the heat capacity the entropy of the solid can also be calculated using  $S = \int \frac{dE}{T} = \int \frac{C}{T} dT$  (Figure 3d). Note that since heat capacity is defined for a constant  $\mathbf{B}$ -field we can construct an entropy curve similar to Figure 3d for each value of the magnetic field.

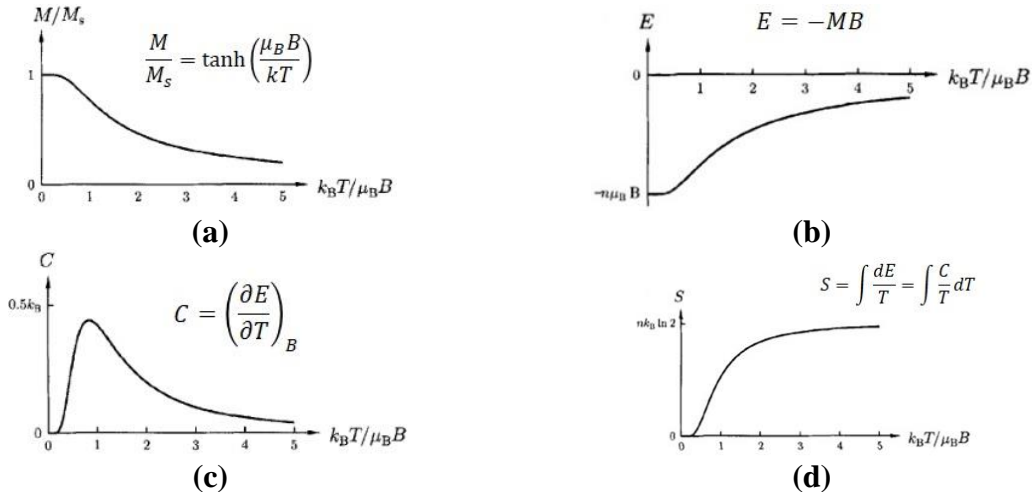


**Figure 3:** (a) magnetisation, (b) energy, (c) heat capacity and (d) entropy curves for a  $J = \frac{1}{2}$  solid

The thermodynamic properties enable a method to cool paramagnetic solids down to extremely low temperatures, as much as a few milli-Kelvin above absolute zero. The procedure is outlined in Figure 4 which shows entropy as a function of temperature for different  $\mathbf{B}$ -fields. The sample is first cooled to a low temperature  $T_i$  (e.g. liquid Helium at 4.2 K) in zero  $\mathbf{B}$ -field (point *a*). Next *isothermal magnetisation* is carried out by switching the magnetic field on. The sample entropy and energy decrease due to alignment of the magnetic moments in the  $\mathbf{B}$ -field (*a*→*b*). Since the process is isothermal the energy is transferred to the thermal bath (e.g. liquid He).

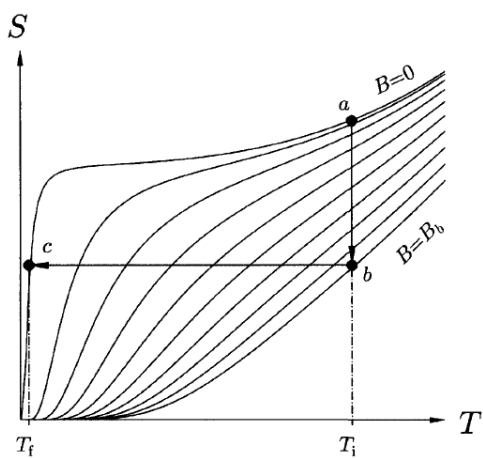


**Figure 4**

The sample is then isolated from its environment to enable the process of *adiabatic demagnetisation*, where the magnetic field is switched off. Since there is no energy transfer the entropy change  $\Delta S = \int \frac{dE}{T} = 0$  is zero (*b*→*c*). The increase in entropy due to spin misalignment under zero  $\mathbf{B}$ -field must therefore be balanced by a simultaneous decrease in entropy caused by phonon annihilation. The destruction of phonons causes the sample temperature to decrease to  $T_f$ , which is lower than  $T_i$ .

## **FoP3B Part I Lecture 8: Exchange interaction and ferromagnetism**

We now move onto solids that display long range ordering of magnetic moments. This is due to a unique quantum mechanical property called **exchange interaction**. After introducing the exchange interaction, we will discuss one type of long range order, known as **ferromagnetism**, which, unlike paramagnetism, results in strongly magnetic solids.

### **Particle Indistinguishability and the Exchange Interaction**

Consider electrons in a small ‘box’ (e.g. an atom) such that their wavefunctions overlap. The electrons are therefore *indistinguishable*. This behaviour is very different to classical physics where point particles are distinguishable. For simplicity let us assume that there are only two electrons in the box, labelled as electrons ‘1’ and ‘2’, and that their wavefunctions are  $\phi_\alpha(\mathbf{r}_1)$  and  $\phi_\beta(\mathbf{r}_2)$ .  $\phi_\alpha(\mathbf{r}_1)$  simply means that electron ‘1’ is in the quantum state  $\alpha$  and similarly for  $\phi_\beta(\mathbf{r}_2)$ . If the two electrons are non-interacting then a possible solution for the total wavefunction  $\Psi(\mathbf{r}_1, \mathbf{r}_2)$  might be  $\phi_\alpha(\mathbf{r}_1)\phi_\beta(\mathbf{r}_2)$ . However, this does not satisfy the condition of indistinguishability, i.e. if  $\mathbf{r}_1$  and  $\mathbf{r}_2$  are swapped in  $\phi_\alpha(\mathbf{r}_1)\phi_\beta(\mathbf{r}_2)$  we do not recover the same electron density ( $|\phi_\alpha(\mathbf{r}_1)\phi_\beta(\mathbf{r}_2)|^2 \neq |\phi_\alpha(\mathbf{r}_2)\phi_\beta(\mathbf{r}_1)|^2$ ). To be consistent with the indistinguishability criterion we can instead propose the following solutions for  $\Psi$ :

$$\begin{aligned}\Psi_s(\mathbf{r}_1, \mathbf{r}_2) &= \frac{1}{\sqrt{2}} [\phi_\alpha(\mathbf{r}_1)\phi_\beta(\mathbf{r}_2) + \phi_\beta(\mathbf{r}_1)\phi_\alpha(\mathbf{r}_2)] \\ \Psi_a(\mathbf{r}_1, \mathbf{r}_2) &= \frac{1}{\sqrt{2}} [\phi_\alpha(\mathbf{r}_1)\phi_\beta(\mathbf{r}_2) - \phi_\beta(\mathbf{r}_1)\phi_\alpha(\mathbf{r}_2)]\end{aligned}$$

The first solution  $\Psi_s$  is a **symmetric wavefunction** since  $\Psi_s(\mathbf{r}_1, \mathbf{r}_2) = \Psi_s(\mathbf{r}_2, \mathbf{r}_1)$ , while  $\Psi_a$  is **anti-symmetric** (i.e.  $\Psi_a(\mathbf{r}_1, \mathbf{r}_2) = -\Psi_a(\mathbf{r}_2, \mathbf{r}_1)$ ). The  $1/\sqrt{2}$  factor is a normalisation constant. The *strong form* of the **Pauli Exclusion principle** states that *the total wavefunction for indistinguishable electrons must be anti-symmetric*. This means that  $\Psi_a$  is a valid wavefunction for electrons, but not  $\Psi_s$ . A consequence of the Pauli Exclusion principle is that electrons cannot have the same quantum state. This is also known as the *weak form* of the Pauli Exclusion principle and follows from the fact that  $\Psi_a(\mathbf{r}_1, \mathbf{r}_2) = 0$  for  $\alpha = \beta$ .

Let us introduce electron spin into the mix. The wavefunction can be broken down into a spatial ( $\psi$ ) and spin-dependent ( $\chi_{\text{spin}}$ ) part, such that  $\Psi(\mathbf{r}_1, \mathbf{r}_2) = \psi(\mathbf{r}_1, \mathbf{r}_2)\chi_{\text{spin}}$ . Due to  $\Psi$  being anti-symmetric (Pauli Exclusion principle) if  $\chi_{\text{spin}}$  is anti-symmetric,  $\psi$  must be symmetric and vice-versa. Consider an anti-symmetric  $\chi_{\text{spin}}$  (i.e. electron spins anti-parallel), so that the spatial part is given by  $\psi_s(\mathbf{r}_1, \mathbf{r}_2) = \frac{1}{\sqrt{2}} [\phi_\alpha(\mathbf{r}_1)\phi_\beta(\mathbf{r}_2) + \phi_\beta(\mathbf{r}_1)\phi_\alpha(\mathbf{r}_2)]$ . The total spin angular momentum  $\mathbf{S} = \mathbf{s}_1 + \mathbf{s}_2$  and the quantum number  $S = \frac{1}{2} - \frac{1}{2} = 0$ . Since  $m_S = S, S-1, \dots, -S$  there is only one quantum state corresponding to  $m_S = 0$ . A suitable wavefunction that satisfies the indistinguishability criterion is  $\frac{|\uparrow\downarrow\rangle - |\downarrow\uparrow\rangle}{\sqrt{2}}$ . This is known as the **spin singlet**, due to the fact that there is only one quantum state. For a singlet  $\psi_s \neq 0$  for  $\mathbf{r}_1 = \mathbf{r}_2$ , i.e. the distance of separation of singlet electrons can be small and hence the average Coulomb interaction energy large.

For  $\chi_{\text{spin}}$  symmetric (i.e. parallel electron spins), the anti-symmetric spatial part is  $\psi_a(\mathbf{r}_1, \mathbf{r}_2) = \frac{1}{\sqrt{2}} [\phi_\alpha(\mathbf{r}_1)\phi_\beta(\mathbf{r}_2) - \phi_\beta(\mathbf{r}_1)\phi_\alpha(\mathbf{r}_2)]$ . The total spin angular momentum quantum number  $S = \frac{1}{2} + \frac{1}{2} = 1$  and consequently there are three degenerate states corresponding to  $m_S = 1, 0, -1$ .

Since there are three states this configuration is known as a spin **triplet**. The wavefunctions are  $|\uparrow\uparrow\rangle$  ( $m_s = 1$ ),  $\frac{|\uparrow\downarrow\rangle+|\downarrow\uparrow\rangle}{\sqrt{2}}$  ( $m_s = 0$ ) and  $|\downarrow\downarrow\rangle$  ( $m_s = -1$ ). For a triplet  $\psi_a = 0$  for  $\mathbf{r}_1 = \mathbf{r}_2$ , i.e. parallel electrons are well separated, so that their Coulomb energy is also lowered.

It is clear that the Pauli Exclusion Principle gives rise to different Coulomb energies depending on the symmetry of the spin wavefunction. This is known as the **exchange interaction energy** and in the **Heisenberg exchange model** takes the form  $-A\mathbf{s}_1 \cdot \mathbf{s}_2$ , where  $A$  is a constant. We have:

$$|\mathbf{S}|^2 = (\mathbf{s}_1 + \mathbf{s}_2)^2 = |\mathbf{s}_1|^2 + |\mathbf{s}_2|^2 + 2\mathbf{s}_1 \cdot \mathbf{s}_2$$

But  $|\mathbf{s}_1|^2 = |\mathbf{s}_2|^2 = s(s+1)\hbar^2 = 3\hbar^2/4$  ( $\because s = 1/2$ ). Similarly,  $|\mathbf{S}|^2 = S(S+1)\hbar^2$ , and is 0 for a singlet ( $S = 0$ ) and  $2\hbar^2$  for a triplet ( $S = 1$ ).  $-A\mathbf{s}_1 \cdot \mathbf{s}_2 = 3A\hbar^2/4$  for a singlet and  $-A\hbar^2/4$  for a triplet. Hence the lowest energy state is determined by the sign of  $A$ . For an atom obeying Hund's rules  $A > 0$  and the triplet with parallel spins is the ground state (Figure 1a). However, for a molecule with covalent bonding the lower energy bonding orbital is symmetric, since electrons must be shared between the two atoms in the molecule.  $\chi_{\text{spin}}$  for the bonding orbital is therefore anti-symmetric and the ground state is a singlet with  $A < 0$  (Figure 1b).

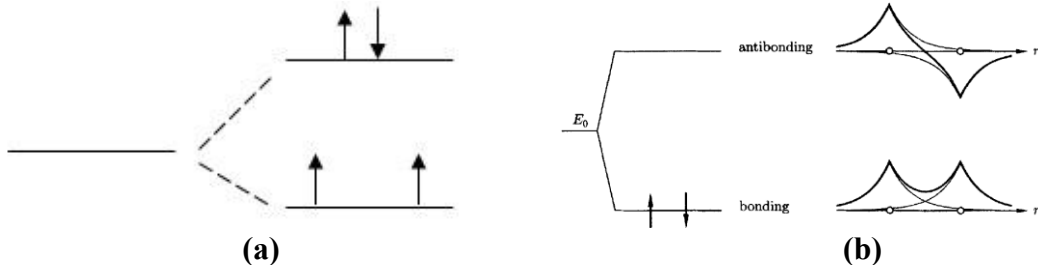


**Figure 1:** energy levels for (a) a single atom and (b) a diatomic molecule.

### Ferromagnetism

If we include exchange the magnetic part of the Hamiltonian becomes:

$$\hat{H}_{\text{mag}} = \sum_{i,j} -J_{ij} \mathbf{S}_i \cdot \mathbf{S}_j + \sum_i \gamma g_J \mathbf{B} \cdot \mathbf{J}_i + \sum_i \frac{e^2}{8m} (\mathbf{B} \times \mathbf{r}_i)^2$$

$J_{ij}$  is the **exchange integral** or **exchange constant** between two atom pairs  $i$  and  $j$ ; it is effectively the constant  $A$  in the previous section. For a ferromagnet  $J_{ij} > 0$ , so that the triplet is the ground state and there is long range *parallel* alignment of spins. Define a molecular field  $\mathbf{B}_{\text{mf}}$  due to neighbouring spins as (the molecular field is not real but instead represents the effects of the exchange interaction):

$$\mathbf{B}_{\text{mf}} = \frac{1}{\gamma g_J} \sum_{j \neq i} -J_{ij} \mathbf{S}_j$$

The molecular field is assumed to be constant at each atom site ' $i$ '. Substituting in the Hamiltonian and assuming identical atoms/ions with  $\mathbf{L} = 0$  and  $\mathbf{J} = \mathbf{S}$  gives:

$$\hat{H}_{\text{mag}} = \sum_i \gamma g_J (\mathbf{B} + \mathbf{B}_{\text{mf}}) \cdot \mathbf{J}$$

where the weaker diamagnetic term has been ignored. The **Weiss model of ferromagnetism** further assumes that  $\mathbf{B}_{\text{mf}} = \lambda \mathbf{M}$ , where  $\mathbf{M}$  is the magnetisation and  $\lambda$  is a constant. The Hamiltonian is similar to a paramagnetic material, but with  $\mathbf{B}$  replaced by  $(\mathbf{B} + \mathbf{B}_{\text{mf}})$  or equivalently  $(\mathbf{B} + \lambda \mathbf{M})$ .

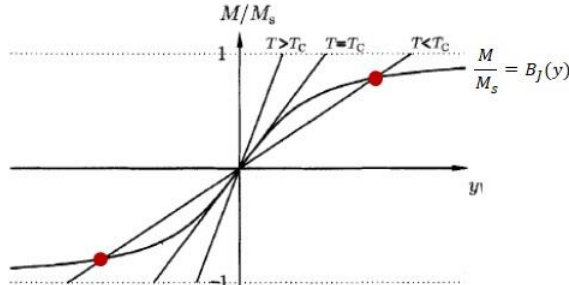


**Figure 2**

Using results derived previously for a paramagnetic solid (Lecture 7):

$$\frac{M}{M_s} = B_J(y) \quad \dots (1)$$

$$y = \frac{g_J \mu_B J (B + B_{\text{mf}})}{kT} = \frac{g_J \mu_B J (B + \lambda M)}{kT} \quad \dots (2)$$

where the Brillouin function  $B_J(y) = \frac{2J+1}{2J} \coth\left(\frac{2J+1}{2J}y\right) - \frac{1}{2J} \coth\left(\frac{y}{2J}\right)$ . Note the inclusion of the molecular field in Equation 2. The magnetisation  $M$  must satisfy Equations 1 and 2 simultaneously. The situation for a zero applied  $\mathbf{B}$ -field is shown in Figure 2. At low temperatures Equation 2 (the straight line in the figure) intersects  $B_J(y)$  at non-zero values of  $M$  (red points), meaning the material has *spontaneous magnetisation* even in the absence of an external magnetic field. The spontaneous magnetisation is due to the internal molecular field.

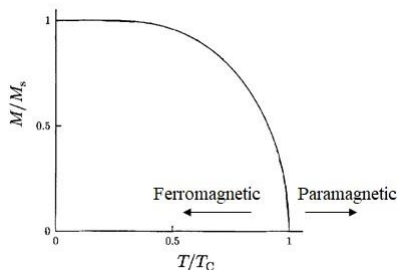


**Figure 3**

The gradient of the  $M$  vs.  $y$  straight line is proportional to temperature (Equation 2). Therefore, at a critical temperature  $T_c$ , called the **Curie temperature**, the spontaneous magnetisation will drop to zero, and the material will be paramagnetic at  $T > T_c$  (Figure 2). The change in magnetisation as a function of temperature is shown in Figure 3; note the *continuous* decrease of  $M$  to zero at  $T=T_c$ .

We can calculate the magnetic susceptibility  $\chi$  of the paramagnetic phase above  $T_c$ . To do this we have to solve Equations 1 and 2 for weak external  $\mathbf{B}$ -fields. The graphical solutions are shown in Figure 4. Note the straight lines representing Equation 2 are now shifted along the horizontal axis due to the applied field; this results in non-zero magnetisation even for  $T > T_c$ .

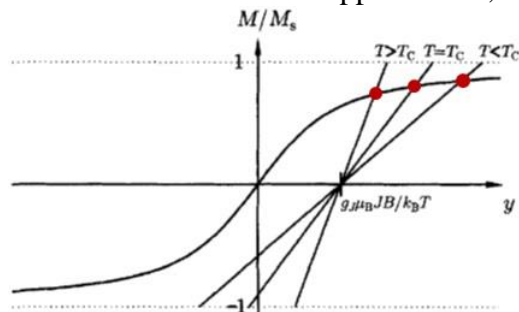


**Figure 4**

For a  $J = 1/2$  solid Equations 1 and 2 give (see also Lecture 7):

$$\frac{M}{M_s} = \frac{\mu_B (B + \lambda M)}{kT} \text{ or } \frac{M}{M_s} \left(1 - \frac{\lambda \mu_B M_s}{kT}\right) = \frac{\mu_B B}{kT}$$

For small magnetisations  $\chi = \mu_0 M/B$  so that:

$$\chi = \frac{\mu_0 \mu_B M_s}{k \left[ T - \frac{\lambda \mu_B M_s}{k} \right]} \propto \frac{1}{T - T_c}$$

For a ferromagnet above  $T_c$  the susceptibility varies as  $\chi \propto 1/(T-T_c)$ ; this is known as the **Curie-Weiss law**. From the expression for  $\chi$  it follows that  $T_c = \frac{\lambda \mu_B M_s}{k}$ . Since  $T_c$  can be measured experimentally we can use this equation to estimate the molecular field at saturation magnetisation  $B_{\text{mf}} = \lambda M_s$ . For ferromagnetic Fe,  $T_c = 1043$  K and the maximum molecular field

is greater than 1,000 Tesla! This is an unimaginably large magnetic field (for reference a field of 1 Tesla is considered to be large). However, we have to bear in mind that  $B_{\text{mf}}$  is not an actual magnetic field and has such a large value because it represents the Coulomb forces between electrons resulting from the exchange interaction.

## FoP3B Part I Lecture 9: Anisotropy and Magnetic Ordering

### Magnetocrystalline anisotropy

The transition metal elements, Fe, Co and Ni are known for their ferromagnetic properties.

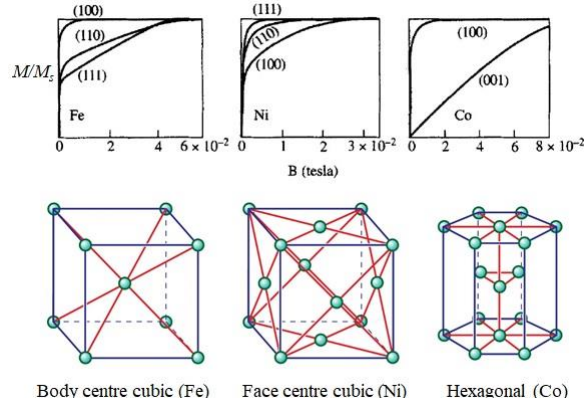


Figure 1

The crystal structure of these elements are all different, with Fe being body centred cubic, Ni face centred cubic and Co hexagonal (Figure 1). It is found that the elements are readily magnetised along certain crystallographic directions than others. For example, for hexagonal Co the **easy** direction of magnetisation is normal to the *basal planes*, i.e. it takes a lower  $\mathbf{B}$ -field to reach saturation magnetisation  $M_s$  along the easy axis compared to other crystal directions (Figure 1).

The reasons for the so-called **magnetocrystalline anisotropy** are somewhat complex. There are ‘crystal field’ effects that arise due to the anisotropic shape of electron orbitals, especially  $d$ -orbitals as found in transition metals, where some electron orbitals are subjected to greater Coulomb repulsion from electrons in neighbouring atoms than others. This results in *orbital quenching* where the net orbital angular momentum  $L = 0$  (note that Hund’s rules for an isolated atom states that  $L$  must be maximised, so orbital quenching is a phenomenon arising from the crystal environment surrounding the atom). The orbital quenching modifies the spin orbit interaction so that the Hamiltonian is now dependent on the crystal direction.

Because of magnetocrystalline anisotropy there is an energy penalty for magnetisation in a direction other than the easy axis. This results in an **energy density** (i.e. energy per unit volume). As an example for hexagonal crystals the energy density is:

$$E = K_1 \sin^2 \theta + K_2 \sin^4 \theta$$

where  $\theta$  = angle between magnetisation direction and easy axis, and  $K_1, K_2$  = anisotropy constants. Note that if magnetisation is along the easy axis  $\theta = 0^\circ$  and there is no energy penalty (i.e.  $E = 0$ ). The above formula is only valid for hexagonal crystals; alternative expressions can be found for crystals of other symmetry, such as, cubic.

### Antiferromagnetism

We will now examine other forms of magnetic moment long range ordering. In ferromagnetism  $J_{ij} > 0$ , so that the triplet has lowest energy, and all the spins are aligned parallel to one another. If  $J_{ij} < 0$  the singlet is the ground state and neighbouring spins are aligned anti-parallel to one another. This form of long range ordering is known as **antiferromagnetism**. An example is MnO, where the spin orientation of magnetic Mn<sup>2+</sup> ions on alternate (111) planes are anti-parallel to one another (Figure 2). Since neighbouring magnetic moments are anti-parallel and are of the same magnitude the *net* magnetisation of an antiferromagnet is zero. In **ferrimagnetism** (e.g. Fe<sub>3</sub>O<sub>4</sub>) the neighbouring spins are anti-parallel, but have different magnitude, resulting in non-zero magnetisation.

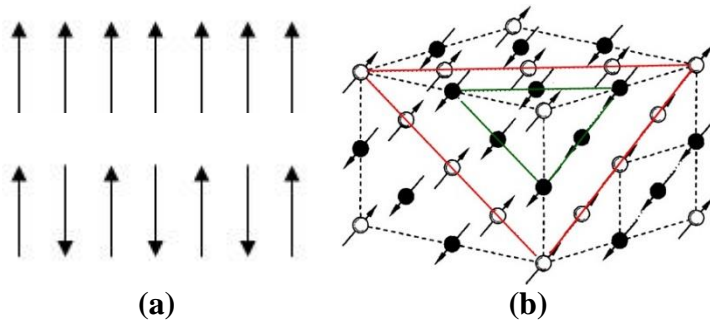


**Figure 2:** (a) ferromagnetic (top) and antiferromagnetic (bottom) spin ordering and (b) the antiferromagnetic solid MnO.

The dark and white circles represent  $\text{Mn}^{2+}$  ions on alternate (111) planes (indicated by the coloured lines).

We can extend the Weiss model of ferromagnetism to antiferromagnets as well. The concept is illustrated in Figure 3, where the antiferromagnetic spin lattice is separated into two ferromagnetic *sub-lattices* (spin up and spin down).

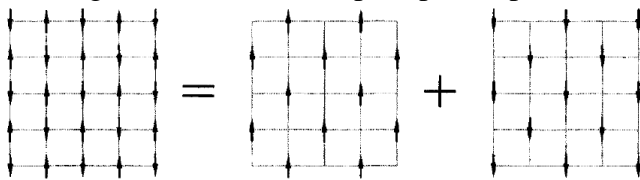


**Figure 3**

Magnetisations on each sub-lattice are equal and opposite. The molecular field imposed by one sub-lattice on the other is given by (+ is spin ‘up’ and – is spin ‘down’):

$$B_{\text{mf}}^+ = -|\lambda|M^-$$

$$B_{\text{mf}}^- = -|\lambda|M^+$$

Note that the molecular field constant is  $-|\lambda|$  rather than  $\lambda$ , since the sign of  $J_{ij}$  for an antiferromagnet is opposite to that of a ferromagnet.

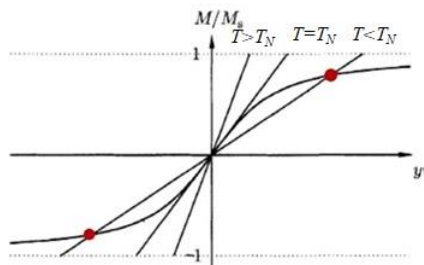


**Figure 4**

Applying Weiss’ theory to a ferromagnetic sub-lattice:

$$\frac{M^\pm}{M_s} = B_J(y^\pm) \dots (1)$$

$$\text{and } y^\pm = \frac{g_J \mu_B J (B + B_{\text{mf}}^\pm)}{kT} = \frac{g_J \mu_B J (B - |\lambda| M^\mp)}{kT} \dots (2)$$

The graphical solution of this problem at zero applied field is shown in Figure 4. The spontaneous magnetisation of a sub-lattice decreases to zero at the **Néel temperature ( $T_N$ )**.

Above the Néel temperature the antiferromagnet becomes paramagnetic. The magnetic susceptibility of the paramagnetic phase can be calculated by solving Equations 1 and 2 under a small applied field  $B$ . The graphical solution is illustrated in Figure 5.

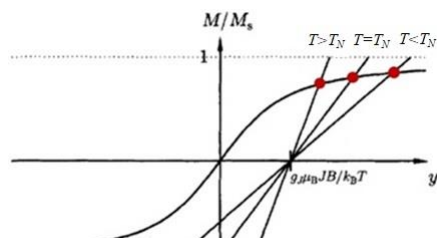


**Figure 5**

For a  $J = 1/2$  solid Equation 1 gives:

$$\frac{M^\pm}{M_s} = \frac{\mu_B(B + B_{\text{mf}}^\pm)}{kT} = \frac{\mu_B(B - |\lambda| M^\mp)}{kT}$$

Since the magnetisation on each sub-lattice is equal in magnitude ( $M^+ = M^- = M$ ):

$$\frac{M}{M_s} \left(1 + \frac{|\lambda| \mu_B M_s}{kT}\right) = \frac{\mu_B B}{kT}$$

For small magnetisations  $\chi = \mu_0 M/B$ :

$$\chi = \frac{\mu_0 \mu_B M_s}{k \left[ T + \frac{|\lambda| \mu_B M_s}{k} \right]} \propto \frac{1}{T + T_N}$$

In general the paramagnetic susceptibility above the transition temperature is found to vary as  $\chi \propto 1/(T - \theta)$ , where  $\theta$  is the **Weiss temperature**. If the material is paramagnetic at low temperature  $\theta = 0$  (Curie's law),  $\theta > 0$  (Curie-Weiss law) for ferromagnetic materials, and  $\theta < 0$  for antiferromagnets.

Since the net magnetisation of an antiferromagnet is zero the question arises what would be the susceptibility below the Néel temperature. In fact, the magnetic susceptibility is different for a **B**-field applied parallel or perpendicular to the magnetisation direction. This is illustrated in Figure 6.

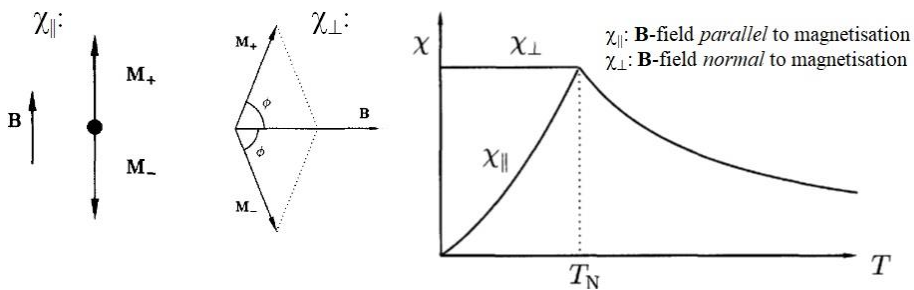


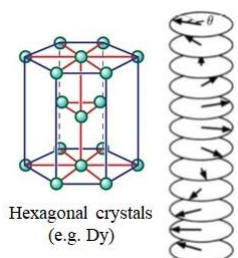
**Figure 6**

The explanation is as follows:

$\chi_{\parallel}$ : At  $T = 0$  K all the spins are perfectly aligned and sub-lattices have saturation magnetisation  $M_s$ . The spin up sub-lattice is favourably aligned with the **B**-field, but not the spin down sub-lattice. Provided the **B**-field is small spin down cannot flip to spin up. Therefore  $\chi_{\parallel}$  is zero at 0 K. Higher temperatures will tend to cause deviations from perfect spin alignment, which can be restored by the applied field, at least for the spin up sub-lattice, causing  $\chi_{\parallel}$  to increase with temperature until  $T_N$ .

$\chi_{\perp}$ : the magnetisation of the two sub-lattices will partly tilt towards the direction of the applied **B**-field. Complete tilting is prevented by the energy penalty due to magnetocrystalline anisotropy.  $\chi_{\perp}$  is approximately independent of temperature below  $T_N$ .

### Helimagnetism



Another form of long range order is **helimagnetism**, where the spin rotates by an angle  $\theta$  between successive planes (e.g. basal planes in hexagonal crystals such as dysprosium Dy; Figure 7). Here the exchange constant between spins in neighbouring ( $J_1$ ) and next-neighbour ( $J_2$ ) planes are important. Let us determine the conditions that favour helimagnetic ordering. The exchange energy term  $-J_{ij}\mathbf{S}_i \cdot \mathbf{S}_j$  is:

**Figure 7**

$$E = -2NS^2(J_1 \cos \theta + J_2 \cos 2\theta)$$

where  $N$  = number of atoms in the plane. The factor of 2 in  $2NS^2$  is due to the fact atom pairs  $i$  and  $j$  are counted twice in  $-J_{ij}\mathbf{S}_i \cdot \mathbf{S}_j$ .

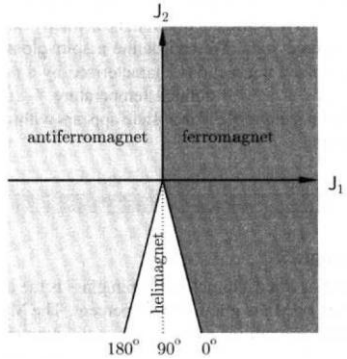


**Figure 8**

The minimum energy condition must satisfy  $dE/d\theta = 0$ , or  $(J_1 + 4J_2 \cos \theta) \sin \theta = 0$ . The solutions are  $\sin \theta = 0$  and  $\cos \theta = -\frac{J_1}{4J_2}$ . The former is satisfied for  $\theta = 0^\circ$  (ferromagnetism) and  $\theta = 180^\circ$  (antiferromagnetism). The latter represents helimagnetism. For an energy minimum  $d^2E/d\theta^2 > 0$  and it is easy to show that for helimagnetism this is satisfied when  $J_2 < 0$ . The helimagnetism stability region is therefore as shown in Figure 8.

## FoP3B Part I Lecture 10: Spin waves and Magnons

The magnetisation of a ferromagnet decreases monotonically with temperature due to increased disorder of the magnetic moments. The Weiss model of ferromagnetism enables us to quantify this change. For a  $J = \frac{1}{2}$  solid,  $\frac{M}{M_s} = B_{1/2}(y) = \tanh y$ , where  $y = \frac{\mu_B \lambda M}{kT}$ . At low temperature  $y \rightarrow \infty$ , so that  $\tanh y = \frac{\sinh y}{\cosh y} = \frac{1-e^{-2y}}{1+e^{-2y}} \approx 1 - 2e^{-2y}$ . Hence:

$$\frac{M}{M_s} = 1 - 2e^{-2y} \text{ or } \frac{M_s - M}{M_s} = 2 \exp\left(-\frac{2\mu_B \lambda M}{kT}\right)$$

Experimentally however it is found that  $M$  decreases faster than the predicted variation. The Weiss model assumes that disorder is created by a full  $180^\circ$  spin flip on some of the atoms (Figure 1a). However, this is a high energy process, and there is an alternative mechanism for generating spin disorder, which also has a lower activation barrier. This is the formation of **spin waves** as shown in Figure 1b.

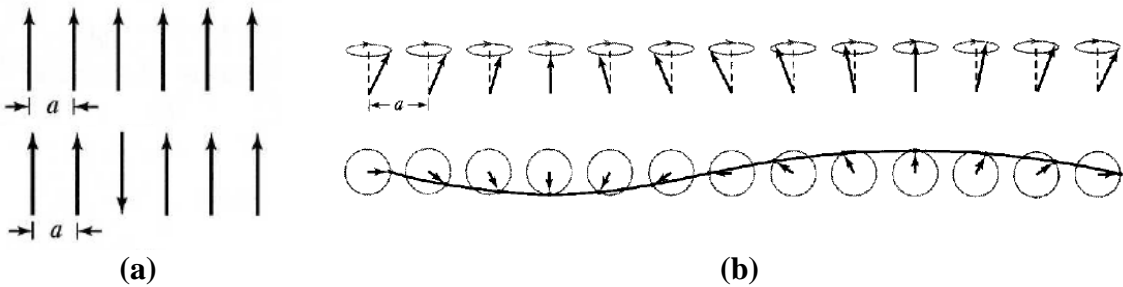


**Figure 1:** (a) spin alignment at  $T = 0$  K (top) and a spin flip at  $T > 0$  K (bottom). (b) a spin wave as viewed from the side (top) and from above (bottom).

### Spin waves and Magnons

Consider a 1D solid of atoms with periodic spacing ' $a$ '. We assume that the exchange interaction is allowed between neighbouring atoms only and has a constant exchange integral  $J_{\text{ex}}$ . Therefore,  $\sum_{i,j} -J_{ij} \mathbf{S}_i \cdot \mathbf{S}_j = \sum_j -2J_{\text{ex}} \mathbf{S}_j \cdot \mathbf{S}_{j+1}$ , where the factor of '2' highlights the fact that an atom pair  $i,j$  is counted twice. The magnetic moment at position ' $j$ ' is  $\boldsymbol{\mu}_j = -g_s \gamma \mathbf{S}_j$  (assuming  $\mathbf{L} = 0$ ). The exchange energy at ' $j$ ' with neighbours ' $j-1$ ' and ' $j+1$ ' is:

$$-2J_{\text{ex}} \mathbf{S}_j \cdot (\mathbf{S}_{j-1} + \mathbf{S}_{j+1}) = -\boldsymbol{\mu}_j \cdot \frac{-2J_{\text{ex}}}{g_s \gamma} (\mathbf{S}_{j-1} + \mathbf{S}_{j+1})$$

The right hand side of the above expression suggests we can define an effective **B**-field ( $\mathbf{B}_{\text{eff}}$ ) at position ' $j$ ' as  $\frac{-2J_{\text{ex}}}{g_s \gamma} (\mathbf{S}_{j-1} + \mathbf{S}_{j+1})$ , based on the fact that the energy of the magnetic moment  $\boldsymbol{\mu}_j$  in a **B**-field is  $-\boldsymbol{\mu}_j \cdot \mathbf{B}$ . The torque ( $\boldsymbol{\tau}$ ) is therefore  $\boldsymbol{\tau} = \frac{d\boldsymbol{\mu}_j}{dt} = \boldsymbol{\mu}_j \times \mathbf{B}_{\text{eff}}$  or:

$$\frac{d\mathbf{S}_j}{dt} = (-g_s \gamma \mathbf{S}_j) \times \frac{-2J_{\text{ex}}}{g_s \gamma} (\mathbf{S}_{j-1} + \mathbf{S}_{j+1}) = 2J_{\text{ex}} [\mathbf{S}_j \times (\mathbf{S}_{j-1} + \mathbf{S}_{j+1})]$$

A more rigorous quantum mechanical derivation shows that (note extra factor  $\hbar$ )\*<sup>1</sup>.

<sup>1</sup> See Supplementary Reading on DUO for a derivation.

$$\frac{d\mathbf{S}_j}{dt} = \frac{2J_{\text{ex}}}{\hbar} [\mathbf{S}_j \times (\mathbf{S}_{j-1} + \mathbf{S}_{j+1})]$$

Let us find solutions to this equation. We assume that the spins are largely parallel to the  $z$ -axis (i.e.  $S^z \approx S$ , where  $S$  is the magnitude of the spin angular momentum), so that the  $x,y$  components,  $S^x$  and  $S^y$ , are small. This results in the following component equations:

$$\begin{aligned}\frac{dS_j^x}{dt} &= \frac{2J_{\text{ex}}S}{\hbar} (2S_j^y - S_{j-1}^y - S_{j+1}^y) \\ \frac{dS_j^y}{dt} &= -\frac{2J_{\text{ex}}S}{\hbar} (2S_j^x - S_{j-1}^x - S_{j+1}^x) \\ \frac{dS_j^z}{dt} &\approx 0\end{aligned}$$

Assume wave-like solutions,  $S_j^x = Ae^{i(qja - \omega t)}$  and  $S_j^y = Be^{i(qja - \omega t)}$  with wavenumber  $q$  and angular frequency  $\omega$ . Substituting in the equations for  $\frac{dS_j^x}{dt}$  and  $\frac{dS_j^y}{dt}$  gives:

$$-i\omega A = \frac{4J_{\text{ex}}SB}{\hbar} [1 - \cos qa] \quad \dots (1)$$

$$i\omega B = \frac{4J_{\text{ex}}SA}{\hbar} [1 - \cos qa] \quad \dots (2)$$

(i) Dividing Equation 1 by 2 gives  $A = iB$ . Since  $i = e^{i\pi/2}$  this implies that there is a  $90^\circ$  phase shift between the  $S^x$  and  $S^y$  component spin waves. In other words, there is a cyclic rotation of the spin in the  $xy$ -plane (Figure 1b).

(ii) Substituting  $A = iB$  in either Equation 1 or 2 gives:

$$\hbar\omega = 4J_{\text{ex}}S(1 - \cos qa)$$

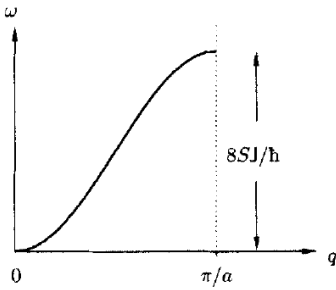


**Figure 2**

For a given wavenumber  $q$  the spin wave can only take a fixed value of energy  $\hbar\omega$ . The dispersion diagram is shown in Figure 2 for the first Brillouin zone. This is similar to the dispersion diagram for *acoustic phonon* waves. In fact, like phonons, spin waves have quantised energies, and can be thought of as quasi-particles called **magnons**.

### Quantum Mechanical Interpretation

As mentioned earlier the activation barrier for a spin wave or magnon is smaller than a full  $180^\circ$  spin flip. Quantum mechanics provides some insight why this might be the case. Denote by  $|0\rangle$  the ground state where all spins are aligned (Figure 3).

$$|0\rangle = \begin{array}{cccccc} \uparrow & \uparrow & \uparrow & \uparrow & \uparrow & \uparrow \\ \rightarrow & a & \leftarrow & & & \end{array}$$

$$|j\rangle = \begin{array}{cccccc} & & j & & & \\ \uparrow & \uparrow & \downarrow & \uparrow & \uparrow & \uparrow \\ \rightarrow & a & \leftarrow & & & \end{array}$$

**Figure 3**

$|0\rangle$  is an eigenstate of the Hamiltonian, i.e.  $\hat{H}_{\text{mag}}|0\rangle = E_0|0\rangle$  where  $E_0$  is the ground state energy. Now define the excited state  $|j\rangle$  as the wavefunction with the spin at site ‘ $j$ ’ flipped (Figure 3). It can be shown that  $|j\rangle$  is not an eigenstate of the Hamiltonian, i.e.  $\hat{H}_{\text{mag}}|j\rangle \neq E_j|j\rangle$  where  $E_j = \text{constant}$ .

In fact, the excited state  $|q\rangle$  that is an eigenfunction of  $\hat{H}_{\text{mag}}$  is a superposition of spin flips spread out over all  $N$ -atoms:

$$|q\rangle = \frac{1}{\sqrt{N}} \sum_{j \in N} e^{iqja} |j\rangle$$

Note also the additional phase term  $e^{iqja}$  accompanying the linear superposition of excited state wavefunctions  $|j\rangle$ . More details leading to the derivation of the above result can be found in the Supplementary Reading on DUO. A spin wave can therefore be interpreted as a *single spin flip* spread out over all atoms. Since the spin flip is delocalised the activation barrier for its formation is small. In fact, for small  $q$ , i.e. long wavelength spin waves, the formation energy  $\hbar\omega$  is vanishingly small (Figure 3). Furthermore, the overall change in spin due to a single flip is  $-\frac{1}{2} - \frac{1}{2} = -1$ . The spin wave is therefore a boson (similar to a phonon).

## FoP3B Part I Lecture 11: Domain Walls

### *Bloch's $T^{3/2}$ law*

Thermal disorder of magnetic moments in a ferromagnet is due to spin waves or magnons. Let us therefore calculate the magnetisation as a function of temperature using a magnon-based model. Excitation of a single magnon will reduce the net magnetic moment by 1 unit. The equilibrium magnon concentration,  $n_{\text{magnon}}$ , therefore determines the magnetisation as a function of temperature. Since magnons are bosons:

$$n_{\text{magnon}} = \int \left[ \frac{1}{\exp\left(\frac{\hbar\omega}{kT}\right) - 1} \right] g_m(\hbar\omega) d(\hbar\omega)$$

where the term within the square brackets is the Bose-Einstein distribution and  $g_m(\hbar\omega)d(\hbar\omega)$  is the density of states, i.e. number of magnon states per unit volume between energy  $E = \hbar\omega$  and  $[\hbar\omega + d(\hbar\omega)]$ . At low temperatures only low energy magnons can be excited. Since the magnon energy  $\hbar\omega = 4J_{\text{ex}}S(1 - \cos qa)$  it follows that  $q$  must be small at low temperature. Using the small angle approximation  $\cos(qa) = 1 - \frac{(qa)^2}{2}$  we have  $\hbar\omega \propto q^2$ . This is a similar energy dependence to electrons in a free electron solid (i.e.  $E \propto k^2$ , where  $k$  is the electron wavenumber). Furthermore, since magnons are also plane waves they satisfy the same boundary conditions as a free electron solid (i.e.  $\mathbf{k} = 2\pi/L$ , where  $L$  is the dimension of the solid). We can use the density of states result from free electron theory to obtain  $g_m(\hbar\omega)d(\hbar\omega) \propto \sqrt{\omega}d(\hbar\omega)$  (see Lecture 1), so that:

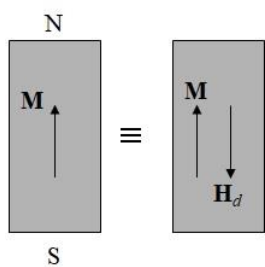
$$n_{\text{magnon}} = \int \left[ \frac{1}{\exp\left(\frac{\hbar\omega}{kT}\right) - 1} \right] g_m(\hbar\omega) d(\hbar\omega) \propto \int_0^\infty \frac{\sqrt{\omega}d\omega}{\exp\left(\frac{\hbar\omega}{kT}\right) - 1}$$

or  $n_{\text{magnon}} \propto \left(\frac{kT}{\hbar}\right)^{3/2} \int_0^\infty \frac{\sqrt{x}dx}{e^x - 1} \propto T^{3/2}$

with  $x = \hbar\omega/kT$ . The magnetisation is then given by  $\frac{M_s - M}{M_s} \propto n_{\text{magnon}} \propto T^{3/2}$ . This is known as **Bloch's  $T^{3/2}$  law**. Experimentally it is found that the magnetisation of a ferromagnet at low temperature obeys Bloch's  $T^{3/2}$  law rather than the Weiss model prediction (see previous lecture). This confirms that spin disorder is due to magnons rather than discrete  $180^\circ$  spin flips.

### **Domain Walls**

We will now discuss **domain walls** in ferromagnetic materials.



Consider a ferromagnetic solid with uniform magnetisation  $\mathbf{M}$  (Figure 1). Since  $\mathbf{B} = \mu_0(\mathbf{H} + \mathbf{M})$  and  $\nabla \cdot \mathbf{B} = 0$ , we have  $\nabla \cdot \mathbf{M} = -\nabla \cdot \mathbf{H}$ . The divergence in  $\mathbf{M}$  is non-zero at the free surfaces, so that a **demagnetising field**  $\mathbf{H}_d$  that is anti-parallel to  $\mathbf{M}$  must be present in order to satisfy Maxwell's equations (Figure 1). Recall however that the energy of a magnetic moment  $\boldsymbol{\mu}$  in a  $\mathbf{B}$ -field is  $-\boldsymbol{\mu} \cdot \mathbf{B}$ . Since  $\mathbf{M}$  and  $\mathbf{H}_d$  are anti-parallel the energy is increased.

**Figure 1**

A ferromagnet minimises this excess energy by forming **domains**. The concept can be illustrated using Figure 2. A solid with uniform magnetisation has magnetic field lines that look like a bar magnet with North-South poles (compare the field lines in Figure 2 (left) with the North-South poles for uniform magnetisation; Figure 1). These magnetic field lines carry excess energy. If we split the solid into two domains with anti-parallel  $\mathbf{M}$  then the field lines, and therefore the excess energy, is reduced somewhat (Figure 2 middle). The lowest energy configuration is shown in Figure 2 (right).

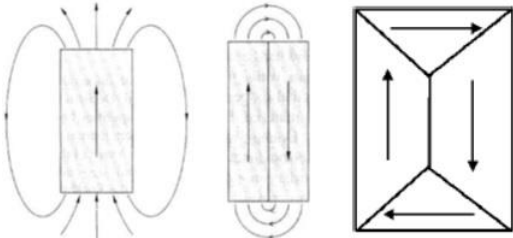


**Figure 2**

Here the domain configuration is such that  $\mathbf{M}$  is parallel to the free surfaces, so that the demagnetising field due to  $\nabla \cdot \mathbf{M} \neq 0$  is avoided. The magnetic field lines outside the solid are absent. The net magnetisation for the entire solid is also zero, but this is a consequence of the domain structure. Within a single domain the magnetisation has the value expected of a ferromagnetic material.

The **domain wall** is the interface separating two neighbouring magnetic domains. On crossing the domain wall the magnetic moments or spins must change their orientation. This process happens gradually over a certain distance. Consider the case where the domain wall is between two neighbouring domains that have anti-parallel spins. As shown in Figure 3 the re-orienting of spins can either happen in a plane parallel to the domain wall (so-called **Bloch walls**) or in a plane perpendicular to the domain wall (**Néel walls**).

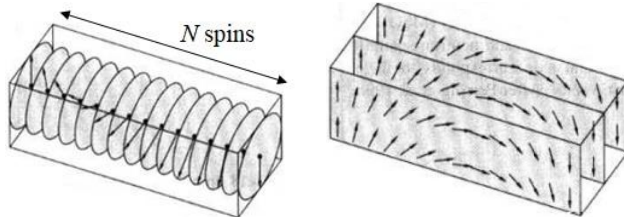


**Figure 3:** Bloch (left) and Néel (right) domain walls

The spin re-orienting happens over  $N$  atoms or  $N$  spins. The value of  $N$  is determined by two opposing factors: exchange energy and anisotropic energy density. Let us examine how these two factors affect the domain wall energy and width.

First consider the exchange energy contribution  $-2J_{\text{ex}}\mathbf{S}_i \cdot \mathbf{S}_j$ . We will assume the atoms have periodic spacing  $a$  in a direction normal to the domain wall, and that the exchange interaction is only present between neighbouring atoms. For  $N$  perfectly aligned spins the energy  $E_0 = -2J_{\text{ex}}NS^2$ . On the other hand, if the spin misalignment between neighbouring atoms is  $\Delta\theta$ , the energy  $E_1 = -2J_{\text{ex}}NS^2 \cos \Delta\theta$ . The energy gain is therefore  $\Delta E = E_1 - E_0 = -2J_{\text{ex}}NS^2(\cos \Delta\theta - 1)$  or  $J_{\text{ex}}NS^2\Delta\theta^2$  for small  $\Delta\theta$  (recall the small angle approximation:  $\cos \Delta\theta \approx 1 - \Delta\theta^2/2$ ). Furthermore,  $N\Delta\theta = \pi$ , so that  $\Delta E \approx J_{\text{ex}} \frac{\pi^2 S^2}{N}$ . The domain wall energy is expressed as an energy per unit area. We can assume that in the plane of the domain wall the spins are arranged in a square lattice (Figure 4a) and that there will be  $(1/a^2)$  spins per unit area. The domain wall energy due to exchange is then  $\sigma_1 = \frac{\Delta E}{a^2} = J_{\text{ex}} \frac{\pi^2 S^2}{Na^2}$ . It follows that the exchange interaction favours a wide domain wall, i.e. large  $N$ .

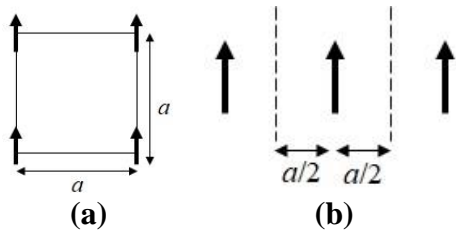


**Figure 4:** Spin arrangement (a) in the plane of the domain wall and (b) along a perpendicular direction to the domain wall.

Next consider the contribution due to the anisotropic energy density, which is assumed to take the form  $K \sin^2 \alpha$  ( $K$  = anisotropy constant,  $\alpha$  = angle w.r.t. easy axis). The anisotropy energy is zero far away from the domain wall (i.e.  $\alpha = 0, \pi$ ). For the intermediate  $N$  spins:

$$\Delta E = \sum_{i=1}^N K \sin^2(i\Delta\theta)$$

Passing onto the continuum limit for small  $\Delta\theta$  and keeping in mind that  $N\Delta\theta = \pi$  gives:

$$\Delta E = \frac{1}{\Delta\theta} \int_0^\pi K \sin^2 \theta d\theta = \frac{N}{\pi} \int_0^\pi K \sin^2 \theta d\theta = \frac{NK}{2}$$

$\Delta E$  is an energy density (i.e. energy per unit volume). The anisotropy energy for a given spin is defined over a distance  $\pm a/2$  in the direction normal to the domain wall (Figure 4b). The anisotropy energy per unit domain wall area is therefore  $\sigma_2 = a\Delta E = \frac{NKa}{2}$ . Note that the anisotropy energy favours a narrow domain wall (i.e. small  $N$ ), unlike the exchange interaction.

The total domain wall energy is  $\sigma = \sigma_1 + \sigma_2 = J_{\text{ex}} \frac{\pi^2 S^2}{Na^2} + \frac{NKa}{2}$ . The equilibrium width is given by the condition  $\frac{d\sigma}{dN} = 0$  which has the solution  $N = \pi S \sqrt{\frac{2J_{\text{ex}}}{Ka^3}}$ . Substituting into the expression for  $\sigma$  we obtain the equilibrium domain wall energy  $\sigma = \pi S \sqrt{\frac{2J_{\text{ex}}K}{a}}$ .

### Magnetic Hysteresis Loops

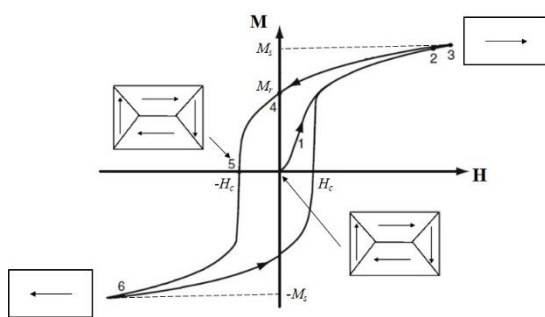


**Figure 5**

The presence of domains gives rise to **hysteresis** behaviour in  $\mathbf{M}$  vs.  $\mathbf{H}$  magnetisation curves (Figure 5). The shape of the hysteresis loop is explained by the energy of individual domains in the presence of an applied magnetic field, i.e. domains where the magnetisation  $\mathbf{M}$  is parallel to  $\mathbf{H}$  have the lowest energy. On reversing the direction of the magnetic field the magnetisation shows hysteresis due to **domain wall pinning** by impurities in the material.

From  $E = -\mathbf{M} \cdot \mathbf{B}$  the area enclosed by a hysteresis loop equals the energy lost during a magnetisation cycle. **Soft magnetic materials** (e.g. Ni-Fe permalloy) have a small hysteresis loop and are therefore used in low power loss applications, such as transformer coils, generators and motors. Soft magnetic behaviour is favoured by wide domain walls (large  $J_{\text{ex}}$ , small  $K$ ),

due to domain pinning being harder. **Hard magnetic materials** (e.g. NdFeB, SmCo alloys) have a large hysteresis loop and are used as permanent magnets for magnetic storage, fridge magnets, loudspeakers etc. They have narrow domain walls (small  $J_{\text{ex}}$ , large  $K$ ), that make domain pinning easier.

.

## FoP3B Part I Lecture 12: Magnetism in Metals

In our discussion of long range magnetic ordering we implicitly assume that spins on neighbouring atoms interact *directly* with one another. In fact, the direct form of the exchange interaction is quite weak. In most cases the exchange interaction proceeds via an intermediary.

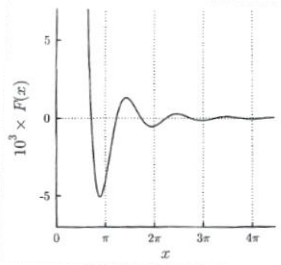


**Figure 1**

For example, in antiferromagnetic MnO magnetic moments on neighbouring Mn<sup>2+</sup> ions interact via O<sup>2-</sup> ions, a process known as *superexchange*. Similarly, in metals the conduction electrons serve as the intermediary in the so-called *RKKY interaction* (named after Ruderman, Kittel, Kasuya and Yosida). The exchange integral for the RKKY interaction has the form  $J_{RKKY}(r) \propto \frac{\cos(2k_F r)}{r^3}$ , where  $k_F$  is the Fermi wavenumber and  $r$  is the distance. Due to the cosine term the RKKY interaction has an oscillatory dependence (Figure 1).

In this final lecture we will look at magnetism in metals. Because the magnetic properties are determined by the conduction electrons we need to develop a *band theory of magnetism*. In particular, we will use these ideas to explore paramagnetism and ferromagnetism in metals. Diamagnetism in metals is slightly more complex and so will not be considered here<sup>1</sup>.

### Pauli Paramagnetism

The theory of paramagnetism in metals is due to Pauli. The density of states  $g(E)$  as a function of energy for the metal in the absence of an applied  $\mathbf{B}$ -field is shown in Figure 2a. The density of states curves for spin up and spin down electrons are shown separately. All the energy levels below the Fermi energy  $E_F$  are filled at absolute zero temperature. Assume a  $J = \frac{1}{2}$  metal with  $\mathbf{L} = 0$  and  $S = \frac{1}{2}$ . Using the fact that  $S_z = m_S \hbar = \pm \frac{1}{2} \hbar$  and  $g_s = 2$  the energy of a single spin in a magnetic field  $\mathbf{B}$  is:

$$-g_s \gamma \mathbf{S} \cdot \mathbf{B} = \mp \gamma \hbar B = \mp \mu_B B$$

Now consider applying a  $\mathbf{B}$ -field parallel to the spin up electrons. The spin down electron energies will increase by  $\mu_B B$ , while the energy of spin down electrons will be lowered by the same amount. Therefore, there is a relative energy shift  $2\mu_B B$  of spin up and spin down bands with respect to one another (Figure 2b). In order to have all energy levels below  $E_F$  occupied at absolute zero the spin down electrons within energy  $\mu_B B$  of  $E_F$  will be transferred to the spin up band (Figure 2b).

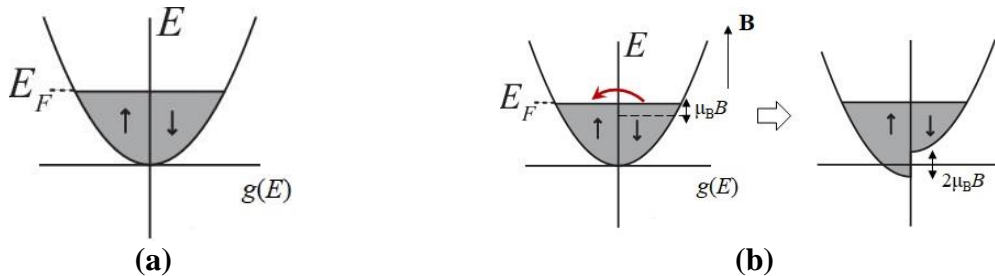


**Figure 2:** Spin up and spin down band structure in the (a) absence and (b) presence of a  $\mathbf{B}$ -field.

<sup>1</sup> The interested student is referred to section 7.6 on ‘Landau diamagnetism’ in Blundell’s book *Magnetism in Condensed Matter*.

Assuming that the density of states at the Fermi energy  $g(E_F)$  does not change significantly within the energy range  $\mu_B B$  (a condition that is valid for small  $B$ ) the change in number of spin down electrons is  $\Delta n \downarrow = -\frac{1}{2}g(E_F)\mu_B B$ . The factor of  $\frac{1}{2}$  is included because  $g(E)$  is the density of states for *all* electrons, spin up and spin down.  $\Delta n \downarrow$  is equal in magnitude to the change in number of spin up electrons, i.e.  $\Delta n \uparrow = -\Delta n \downarrow = \frac{1}{2}g(E_F)\mu_B B$ . The magnetisation  $M = \mu_B(\Delta n \uparrow - \Delta n \downarrow) = g(E_F)\mu_B^2 B$ . For small magnetic fields the susceptibility  $\chi$ :

$$\chi = \frac{M}{H} \approx \frac{\mu_0 M}{B} = g(E_F)\mu_0\mu_B^2$$

For a free electron metal the electron energy  $E = \frac{(\hbar k)^2}{2m}$  and  $\frac{dE}{dk} = \frac{\hbar^2 k}{m}$ . Therefore:

$$g(E)dE = 2 \frac{4\pi k^2}{(2\pi)^3} \frac{dk}{dE} dE = \frac{mk}{\pi^2 \hbar^2} dE$$

From lecture 1 the electron density  $n = (k_F^3/3\pi^2)$  so that:

$$g(E_F) = \frac{mk_F}{\pi^2 \hbar^2} = \frac{mk_F^3}{\pi^2 (\hbar k_F)^2} = \frac{3n}{2E_F}$$

Substituting in the expression for susceptibility gives:

$$\chi = g(E_F)\mu_0\mu_B^2 = \frac{3n\mu_0\mu_B^2}{2E_F}$$

Note that  $\chi$  for Pauli paramagnetism is temperature independent, unlike the result for *localised* magnetic moments (Lecture 7) which predicted  $\chi \propto 1/T$  (Curie's law).

### Ferromagnetism and the Stoner criterion

In ferromagnetism we have an internal molecular field  $\mathbf{B}_{mf}$  even in the absence of an external magnetic field. Let us assume that the direction of  $\mathbf{B}_{mf}$  is parallel to spin up electrons.

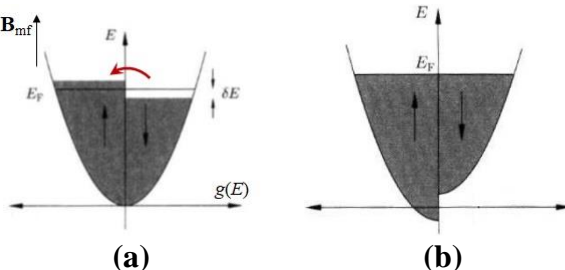


**Figure 3**

For a *spontaneous* magnetisation to take place spin down electrons within energy  $\delta E$  of  $E_F$  must be transferred to the spin up band. Two competing effects must however be taken into consideration: (i) increase in kinetic energy of transferred electrons (Figure 3a) and (ii) decrease in potential energy (Figure 3b).

Let us first consider the kinetic energy increase which is given by (the term within the curly brackets is the number of electrons transferred; Figure 3a):

$$\Delta E_{KE} = \left\{ \frac{1}{2} g(E_F) \delta E \right\} \delta E = \frac{1}{2} g(E_F) (\delta E)^2$$

Using the relation<sup>2</sup>  $dE = -\mathbf{B}(\mathbf{M}) \cdot d\mathbf{M}$  the potential energy decrease due to the molecular field  $B_{\text{mf}} = \lambda M$  is:

$$\Delta E_{PE} = - \int_0^M \lambda M' dM' = -\frac{\lambda M^2}{2}$$

From the previous analysis of paramagnetism the magnetisation:

$$M = \mu_B (\Delta n \uparrow - \Delta n \downarrow) = g(E_F) \mu_B \delta E$$

where the substitution  $\delta E = \mu_B B$  has been made.  $\therefore \Delta E_{PE} = -\frac{\lambda M^2}{2} = -\frac{1}{2}(\lambda \mu_B^2)[g(E_F)\delta E]^2$ . The term  $U = \lambda \mu_B^2$  is called the **Coulomb energy**, since it depends on  $\lambda$  and hence the molecular field which gives rise to the (Coulomb-based) exchange interaction. The net change in energy is therefore:

$$\Delta E = \Delta E_{KE} + \Delta E_{PE} = \frac{1}{2} g(E_F)(\delta E)^2 [1 - Ug(E_F)]$$

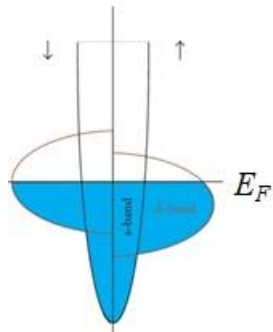


**Figure 4:** density of states of *s* and *d*-bands

For ferromagnetism  $\Delta E < 0$ , which leads to the **Stoner criterion**  $Ug(E_F) > 1$ . This condition predicts that ferromagnetism is favoured by a large Coulomb interaction ( $U$ ) and/or a high density of states at the Fermi level. The latter condition means ferromagnetism is more likely in transition metals (e.g. Fe, Co, Ni) where  $g(E_F)$  is large due to a narrow energy *d*-band (Figure 4). This means that electrons can be transferred from the low potential energy spin band without significantly increasing the kinetic energy of the transferred electrons.

---

<sup>2</sup> The equation  $dE = -\mathbf{B}(\mathbf{M}) \cdot d\mathbf{M}$  is slightly different to the more familiar expression  $-\mathbf{M} \cdot \mathbf{B}$  we have come across before for a fixed magnetisation  $\mathbf{M}$  in a magnetic field. The difference is due to the fact that the molecular  $\mathbf{B}$ -field is now a function of  $\mathbf{M}$  (i.e.  $\mathbf{B}_{\text{mf}} = \lambda \mathbf{M}$ )